Original Contribution

Kurume Medical Journal, 54, 77-84, 2007

Influence of Angiogenesis by Implantation of Bone Marrow Mononuclear Cells in the Rat Ischemic Heart

YOSHINORI YOKOKURA, NOBUHIKO HAYASHIDA, TEIJI OKAZAKI, EIJI NAKAMURA, EIKI TAYAMA, HIDETOSHI AKASHI AND SHIGEAKI AOYAGI

Department of Surgery, Kurume University School of Medicine, Kurume 830-0011, Japan

Received 21 September 2007, accepted 16 January 2008

Summary: Bone marrow implantation (BMI) enhances angiogenesis in several animal models of ischemic diseases, and it is currently applied in the clinical treatment of humans. However, the mechanisms of this effect have not yet been fully described. Rat bone marrow mononuclear cells (BM-MNCs) were obtained by Histopaque density gradient centrifugation and injected directly into the ischemic myocardium of the test rats (BMI group), which were then examined and compared with the groups that received surgery only (Controls) or surgery and an injection of phosphate buffered saline (PBS group). Cardiac function was evaluated by echocardiography, and neovascularization was examined both histologically and immunohistochemically before, 1 day after, and 7 or 28 days after the operation. BM-MNCs were analyzed by fluorescence staining for the endothelial cell marker CD31 and alkaline phosphatase (ALP). The mechanisms of angiogenesis were examined by gene expression analysis. In the BMI group, cardiac function parameters at 7 days after operation were significantly improved and the number of capillaries in the myocardium was significantly larger than that in the PBS and Control groups. Gene analysis showed the expression of 12 genes in the BMI group 7 days after operation. The implantation of BM-MNCs into the myocardiumin cases of acute infarction enhances cytoprotection and angiogenesis by affecting gene expression.

Key words animal model, angiogenesis, ischemic heart disease

INTRODUCTION

Bone marrow mononuclear cells (BM-MNCs) have many of the characteristics of stem cells with respect to mesenchymal tissues [1], and contain numerous kinds of primitive cells which can differentiate into hematopoietic cells and endothelial progenitor cells [2]. Several researchers have suggested that the transplantation of bone marrow cells into ischemic tissue may enhance collateral perfusion via the supply of angioblasts and angiogenic ligands [3,4]. Shintani et al. [5] showed that the direct local transplantation of autologous BM-MNCs can be a useful strategy for therapeutic neovascularization of ischemic tissues. More recently, this technique was applied clinically and remarkable therapeutic effects were demonstrated in patients with myocardial infarction [6,7]. On the other hand, it has been reported that numerous factors including vascular endothelial growth factor and basic fibroblast growth factor are associated with the augmentation of angiogenesis [8]. The exact mechanisms of this angiogenesis remain to be clarified.

In the present study, the histological and functional angiogenic effects of BM-MNC implantation were evaluated in a rat ischemic heart model, and the mechanisms of angiogenesis were examined by gene expression analysis.

Corresponding author: Yoshinori Yokokura, MD, Department of Surgery, Kurume University School of Medicine, 67 Asahi-machi, Kurume 830-0011, Japan. Tel: +81-942-35-3311 Fax: +81-942-35-8967 E-mail: ynoriy@med.kurume-u.ac.jp

Abbreviations: BMI, bone marrow implantation; BM-MNCs, bone marrow mononuclear cells; DNA, deoxyribonucleic acid; EF, ejection fraction; LVDd, left ventricular end-diastolic; LVDs, left ventricular end-systolic diamete; MI, myocardial infarction; PBS, phosphate buffered saline; RNA, ribonucleic acid.

MATERIALS AND METHODS

This study was approved by the Institutional Animal Care and Use Committee of the Kurume University School of Medicine. All animals received human care in compliance with the European Convention on Animal Care.

Study Group

Male inbred Lewis rats (age: 8-10 weeks old, body weight: 230-260 g) were randomized into the following 3 groups: (i) Controls (n=12), the myocardial infarction (MI) group, in which the rats underwent left anterior descending artery (LAD) ligation only; (ii) the PBS group (n=20), in which 50 μl of phosphate buffered saline (PBS) was injected at 4-6 points in the border zone between myocardial infarction and the intact tissue, after operation using a 29-gauge needle; and (iii) the bone marrow implantation (BMI) group (n=20), in which a total of 5×10^6 bone marrow cells (BMCs) in 50 μl of PBS was injected in the same manner as for the PBS group.

Preparation of the acute myocardium rat model

Rats were intraperitoneally anesthetized with 50 mg/kg of pentobarbital and intubated with a 16-French intravenous catheter. They were then placed on a volume ventilator (SAR-830/AP small animal ventilator; CWE, Inc., Ardmore, PA, USA) and ventilated with room air at a tidal volume of 10 ml/kg and at a rate of 80 strokes/min. Left thoracotomy was performed through the fourth intercostals space and the LAD was ligated with 7-0 nylon sutures. The lung was expanded and the chest and thoracotomy incisions were closed after the treatment [9,10].

Preparation of rat bone marrow cells

BMCs were harvested from the male inbred Lewis rats by washing tibias and femurs with Dulbecco's PBS. Bone marrow cell suspension was prepared by gently pressing the bone marrow segments through a fine nylon mesh. The mononuclear cells were then isolated by centrifugation through a Histopaque density gradient centrifugation as described previously by Asahara et al. [11].

Cell characterization

The BM-MNCs were analyzed by fluorescence staining for the endothelial cell marker CD31 (BD PharMingen, (Franklin Lakes, NJ, USA) [12]. The cells were analyzed using a fluorescence-activated cell sorter (FACS) (BD FACS Aria; BD Biosciences, San Jose, CA, USA). Approximately 10,000 cells were screened and the data were expressed as a percentage of positive cells relative to the total cell number.

The cells were cultured on gelatin-coated plates in Medium 199 with 20% fetal bovine serum (FBS), endothelial cell growth supplement, heparin 10 U/ml and antibiotics (Gibco, Gaithersburg, MD, USA) at 37°C under 5% CO_2. Cultures were examined for the development of cell clusters, which is the typical morphological appearance of endothelial precursor cells. On day 7 of culture, we added DiI-acetylated low-density lipoprotein (acLDL) in the culture plate, and observed it 6 hrs later. [5,6,11]

Bone marrow implantation

Immediately after operation, rats with myocardial infarction underwent BM-MNC implantation. After anesthetization with 50 mg/kg of pentobarbital, a total of 5×10^6 BMCs in 50 μl of phosphate buffered saline (PBS) was injected intramuscularly at 4-6 points in the border zone between the myocardial infarction and the intact tissue using a 29-gauge needle in BMI group. The PBS group received an injection of 50 μl of PBS alone.

Monitoring of the implanted cells in the myocardium with infarction

To determine whether the injected BMCs remained in the border zone between the myocardial infarction and the intact tissue, suspended BMCs were labeled with intracellular fluorescent 5(6)-carboxyfluorescein diacetate succinimidyl ester (CFSE) dye prior to implantation into the infarction and surrounding zone as described by Fujioka et al. [14]. Briefly, purified BMCs were resuspended in PBS containing 20 mmol/l CFSE and incubated for 10 min at 37°C with gentle mixing. After washing 3 times with PBS, the labeled BMCs were injected into the ischemic heart model that was prepared together with the 3 groups used in the present study. The rats were examined using the same procedure for all 3 groups; specifically, their hearts were extracted 7, embedded in optimal cutting temperature (OCT) compound (Tissue-TeK; Ted Pella, Inc., Redding, CA, USA) and snap frozen in liquid nitrogen. The tissue was cut into 5 μm-thick sections and examined by fluorescence microscopy in order to detect the labeled cells [15].

Echocardiography

Transthoracic echocardiography was performed

in the 3 groups under general anesthesia with a 5.0-MHz phased array transducer (ALOKA SSD-5500B; High Technology, Inc., Walpole, MA, USA) before, 1 day after, and 7 or 28 days after the operation. Left ventricular end-diastolic (LVDd) and left ventricular end-systolic diameter (LVDs), ejection fraction (EF), and anterior and posterior wall thickness during the systolic phase were measured in the short axis view at the mid-papillary muscle level. Measurements of 3 consecutive cardiac cycles were averaged and examined.

Immunohistochemistry

Immunohistochemical analysis was performed 7 and 28 days after the operation. Myocardial tissue samples were collected around the infarction zone, embedded in optimal cutting temperature (OCT) compound, snap-frozen in liquid nitrogen, and cut into 5 μm-thick sections. The sections were stained with alkaline phosphatase (ALP) and immunostained with mouse anti-rat CD31 monoclonal antibody. Capillary density was histologically examined in 5 randomly selected fields in the area around the zone of the left ventricular myocardium. Capillaries were identified as tubular structures that were positive for CD31and ALP.

mRNA expression and microarray analysis

Cardiac tissues for mRNA expression and microarray analyses were examined using 2 samples each from the BMI and PBS groups. Myocardial tissues were obtained 7 days after operation from the resected heart chamber that had been sufficiently irrigated with 4°C PBS injected from the inferior vena cava under anesthesia. The tissue around the infarction zone corresponding to the implantation site was placed on ice, promptly soaked in RNA stabilization solution (RNAlater; Ambion, Inc., Austin, TX, USA), and maintained at –20°C until use.

Five μg of the isolated total RNA was utilized for the synthesis of double-stranded (ds) cDNA using a one-cycle cDNA synthesis kit (Affymetrix, Santa Clara, CA, USA). Biotin-labeled cRNA was then prepared using a GeneChip IVT Labeling Kit (Affymetrix). The purified cRNA was fragmented by incubation in fragmentation buffer at 94°C for 35 min and chilled on ice. The fragmented and labeled cRNA was applied to Rat Expression Array 230A (Affymetrix), which contains approximately 15,000 rat gene probes, hybridized to the probes in the array, and washed and stained following the manufacturer's instructions (GeneChip Expression Analysis Technical Manual). Probe arrays were scanned using an Agilent GeneArrays Scanner (Agilent Technologies, Palo Alto, CA, USA), and the readings from the quantitative scanning at 570 nm were analyzed by Affymetrix Microarray Suite version 4.0. For the comparisons, hybridization intensities were calculated using a global scaling intensity of the top 100 known genes.

RESULTS

Cell characteristics

BM-MNCs were isolated and analyzed using a FACS. BMCs produce endothelial progenitor cells. In

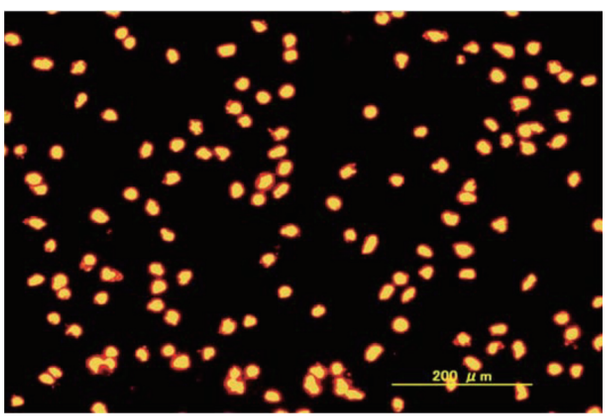

Fig. 1. Incubated bone marrow cells of rats. Cell clusters were found to incorporate DiI-acetylated LDL (acLDL), which is a characteristic function of endothelial cells and endothelial progenitor cells.

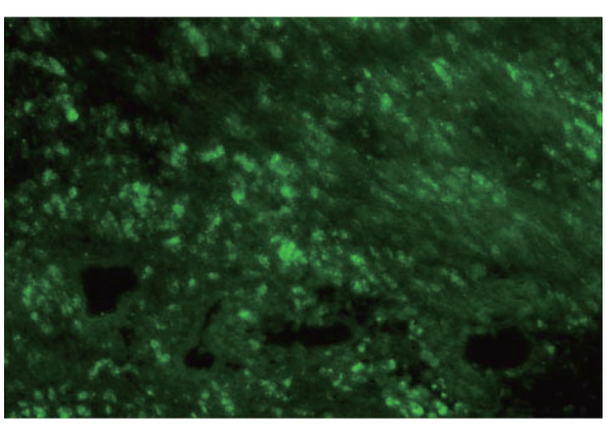

Fig. 2. Fluorescence photomicrograph of a cross-section of the border zone between the myocardial infarction and the intact tissue that had been injected with 5(6)-carboxyfluorescein diacetate succinimidyl ester (CFSE)-labeled bone marrow cells. Cells appeared in the infarction zone 7 days after injection.

1×10^6 BM-MNCs, 18.18% of the endothelial progenitor cells were positive for CD31, a cell clusters and attaching cells (AT cells) appeared within 1-3 days. The AT cells formed linear cord-like structures and multiple cell clusters, and incorporated DiI-acetylated LDL (acLDL); these are characteristic functions of endothelial cells and endothelial progenitor cells (Fig. 1).

Implanted cells

CFSE-labeled BMCs were examined by fluorescence microscopy. At post-BMI days 1 and 7, CFSE-labeled BM-MNCs were observed in the border zone between the myocardial infarction and the intact tissue of the myocardium (Fig. 2).

Cardiac function

Echocardiographic assessments of left ventricular

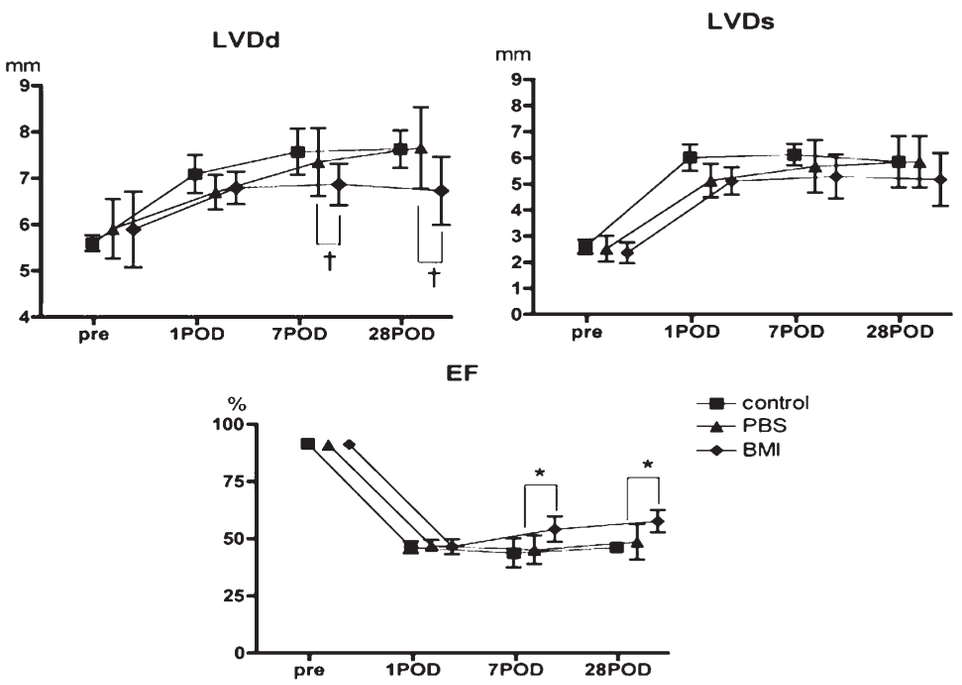

Fig. 3. Left ventricular end-diastolic diameter (LVDd) and systolic (LVDs) diameters, and ejection fraction (EF) in the 3 groups. One day after implantation, the levels in all 3 groups were higher (LVDd) or lower (EF) than pre-infarction levels. At 7 and 28 days after implantation, LVDd values in the bone marrow implantation (BMI) group were lower and EF was higher than in the phosphate buffered saline (PBS) and Control groups.

*p<0.01, †p<0.05

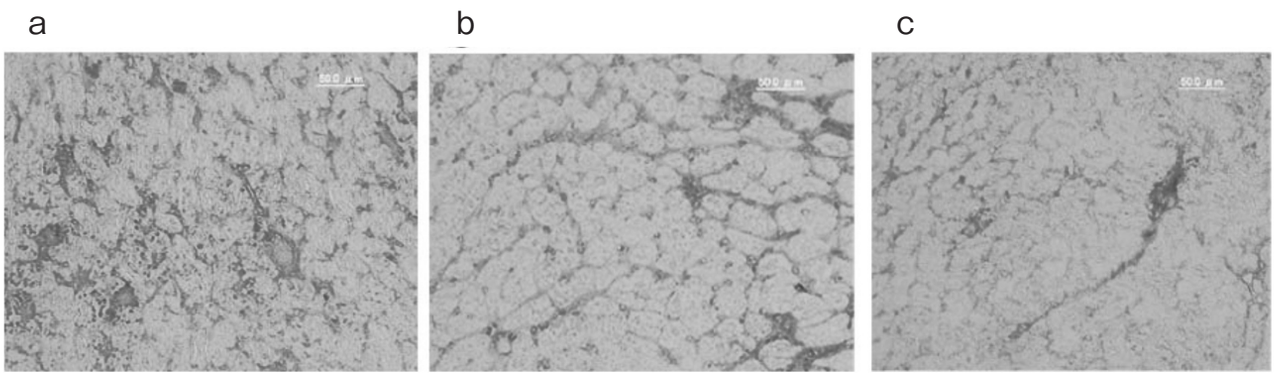

Fig. 4. Effect of BMI on neovascularization. Vascular endothelial cells were stained with CD31. Light photomicrographs of a cross-section of the infarcted myocardium in the BMI (a), the PBS (b), and the Control (c) groups at 28 days post-transplantation. The circular formations stained in brown are the blood vessels.

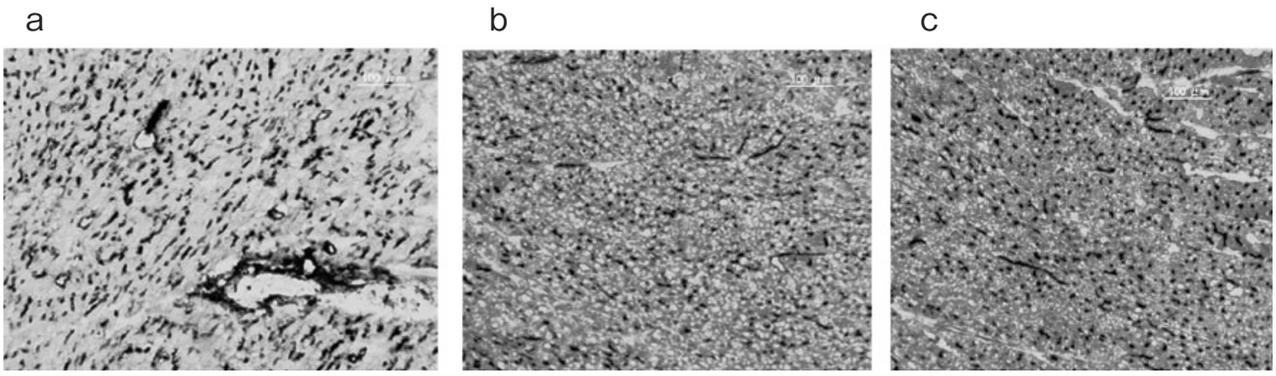

Fig. 5. Effect of BMI on neovascularization. Vascular endothelial cells were stained with alkaline phosphatase (ALP). Light photomicrographs of a cross-section of the infarcted myocardium in the BMI (a), PBS (b), and the control (c) groups at 28 days post-transplantation. The circular formations stained in dark blue are the blood vessels.

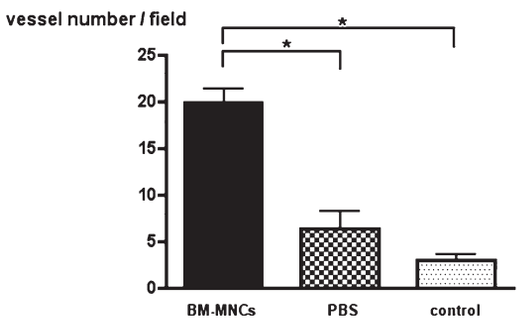

Fig. 6. Capillary density in the rat ischemic myocardium 14 days after transplantation. Density was significantly high in the BMI group. *$p<0.01$.

function (LVDd, LVDs and EF) are shown in Fig. 3. Cardiac function was found to be depressed 1 day after operation in all groups. LVDd and EF in the BMI group, however, had improved significantly at 7 and 28 days after operation.

Microvessels in the myocardium

The immunohistochemical staining results of CD31 and ALP in the infarcted myocardium are shown in Figs 4 and 5, respectively. The density of microvessels in the area around the infarction zone was significantly higher in the BMI group than in the PBS and Control groups at 28 days after implantation (Fig. 6).

Gene expression

Several alterations in gene expression were found in the BMI group in comparison to the PBS group (n=2 each). The genes with a relatively high frequency of alteration in all 4 examined samples, i.e., genes related to cell proliferation signals (Per2, Gnaq, Btc), oxidative stress (Cype2e 1, Mt1a) and transcription factor (Znf498_predicted, Dhx9_predicted, Nr1d1, Bhlhb3, Dbp, Olfm3, Ephxl) are summarized in Table 1.

DISCUSSION

BM-MNCs were injected around the area made ischemic by direct ligation in a rat myocardial infarction model, and their effects were compared to those observed in cases with PBS injection or in cases of myocardial infarction only. Regardless of the treatment, the animals died due to the infarction, however, the injection of BM-MNCs was found to suppress left ventricular dilatation and improve left ventricular contractility. In the chronic ischemic stage (post-BMI 7 and 28 days), angiogenesis was observed in the proximal area of the infarction zone. Gene analysis of the tissues around the infarction zone on post-operative day 7 using gene chips showed the appearance of genes related to transcription, signaling and anti-oxidative stress. To date, the mechanisms of angiogenesis due to cell implantation remains unknown, however, the present findings of gene expression in the implantation zones is an indication that such a mechanism may exist. Though the role and actions of the genes found in our analysis have not yet been fully clarified, these genes are expected to be involved in angiogenesis.

After Asahara et al. [11] reported that vascular endothelial progenitor cells were present in the bone marrow and peripheral blood of humans, therapeutic angiogenesis in which BM-MNCs and peripheral monocytes are transplanted to ischemic tissues has been conducted both experimentally and clinically.

TABLE 1.
Genes with altered expression in the BMI group in comparison to the PBS group
Signal ratio (BMI group/PBS group) is shown as a log_2 number

Functional cluster	Gene name	Gene symbol	Gene bank accession	Signal Log_2 ratio
GTPase activity signal transducer	guanine nucleotide binding protein, alpha q polypeptide	Gnaq	AW143805	2.72
Receptor binding epidermal growth factor	betacellulin	Btc	NM022256	1.85
Signal transducer activity	period homolog 2 (Drosophila)	Per2	NM031678	2.17
Monooxygenase activity	cytochrome P450, family 2, subfamily e, polypeptide 1	Cyp2e1	NM031543	2.61
Metal ion binding	metallothionein	Mt1a	AF411318	1.84
Transcription factor	zinc finger protein 498 (predicted)	Znf498_predicted	BE104397	2.35
DNA binding RNA polymerase Ⅱ transcription	D site albumin promoter binding protein	Dbp	AI230048	2.98
Nucleic acid binding	DEAH (Asp-Glu-Ala-His) box polypeptide 9 (predicted)	Dhx9_predicted	BF398414	1.68
DNA binding transcription factor activity	nuclear receptor subfamily 1, groupD, member 1	Nr1d1	M25804	2.83
Aminopeptidase activity	epoxide hydrolase 1	Ephx1	NM012844	1.65
DNA binding transcription factor activity	basic helix-loop-helix domain containing, class B3	Bhlhb3	NM133303	1.63
Protein binding	olfactomedin 3	Olfm3	AF442822	5.16

Peripheral monocytes are easily collectable [16], but the obtainable number is not large. BM-MNCs are obtainable in large numbers, and contain many undifferentiated cells related to angiogenesis, such as endothelial progenitor cells, as well as progenitor cells that are not related to blood vessels, e.g., fat and bone cells [17]. This point has been suggested to be a cause of ectopic calcification and other problems at cell transplantation [18]. In the present study, we obtained BM-MNC fraction with a high rate of endothelial progenitor cells by Histopaque density gradient centrifugation (Fig. 2) [5]. On post-operative 7 day, many CFSE-labeled cells were observed in the area around the infarction zone where the BM-MNCs had been implanted, but there was no ectopic calcification. Thus, BM-MNC implantation is safe for therapeutic angiogenesis when the rate of endothelial progenitor cells in BM-MNCs is high.

Echocardiography showed that BM-MNC implantation resulted in the suppression of left ventricular dilatation and in significantly good recovery of left ventricular contractility. Thus, the present implantation achieved partial recovery of cardiac function and suppression of the remodeling of the infarction zone, which is consistent with in the results of previous studies [10,19].

The present immunohistochemical results demonstrate that the implanted CFSE-labeled cells had adhered to the tissues around the infarction zone, and that capillary density was high in the BMI group. The implantation of BM-MNCs is thus believed to enhance angiogenesis, and then to promote the suppression of post-infarction remodeling in the myocardium and the improvement of cardiac function.

On the other hand, different mechanisms of angiogenesis due to cell implantation are possible: (i) implanted cells such as endothelial progenitor cells are directly incorporated into the vascular system, and induce vasculogenesis and angiogenesis, or (ii) implanted cells secrete angiogenic factors and inflammatory cytokines, and induce angiogenesis. Therefore, in order to clarify the actual mechanism of angiogenesis by BM-MNC implantation, it is necessary to analyze not only the expression of related genes in the treated zone, but also the comprehensive gene expression profile. In the present study we conducted gene analysis using gene chip technology, which permits expression analysis of approximately 30,000 genes. In addition to the known angiogenic factors, several genes (see below) were found to be expressed at twice or higher levels in the BMI group compared to the PBS group, and this high expression was thought to be attributable to the cell implantation.

The guanine nucleotide binding protein, alpha q polypeptide (Gnaq) is one of the G proteins, such as Type 1 receptor of angiotensin Ⅱ and endothelin receptor, that are involved in various transmembrane signaling systems. The increase of Gnaq expression observed in the BMI group could be associated with suppressed post-infarct remodeling and with the improvement of cardiac function through an increase in heart contractility and myocardial hypertrophy. In addition, increased Gnaq expression is thought to be involved in the promotion of angiogenesis because angiotensin Ⅱ promotes the restoration of ischemic vessels [20].

Betacellulin (Btc) is a member of the epithelial growth factor family that regulates cell cycles [15]. This gene is involved in the proliferation of vascular smooth muscle cells, and its increased expression could promote angiogenesis.

Metallothionein (Mtla) is reported to induce antioxidative activity, and hormones and cytokines regulate its expression [21]. In the heart, Mtla expression is thought to correspond to oxidative stress due to myocardial infarction [21]. In the present study, its expression was found to have increased after the implantation of BM-MNCs, and expression was thought to be up-regulated as a defense system against oxidative stress due to myocardial infarction.

The expression of Zinc finger protein 498 (Znf498-predicted) [22], a transcription factor related to angiogenesis and growth, was also increased in the BMI group, which was thought to be the result of the implantation.

An additional 4 genes expressed in the present study are period homolog 2 (Per2); D site albumin promoter binding protein (Dbp); nuclear receptor subfamily 1, group D, member 1 (Nr1d1); and basic helix-loop-helix domain containing, class B3 (Bhlhb3). These genes are thought to be related to circadian rhythm, but their involvement in angiogenesis remains unknown at the time of writing. The other genes expressed in the present study were DEAH box polypeptide 9 (Dhx_9predicted), epoxide hydrolase 1 (Ephx1) and olfactomedin 3 (Olfm3). To the best of our knowledge, their role and functions in angiogenesis and other processes are completely unknown. Future studies are needed to investigate how and whether the combined expression of these genes relate to angiogenesis in the myocardium and to the improvement of cardiac function.

Comparison and evaluation with gene chip technology is extremely useful in studies on unknown mechanisms in tissues in which implantation is expected to have certain effects. In the present study, the number of rats for gene analysis was limited and the sample timing was not optimized. These issues must be addressed in future studies, and the specificity and quantification of the expressed genes must also be examined by reverse transcriptase-polymerase chain reaction (RT-PCR) and Northern blot analysis. More detailed investigations on the functions of these expressed genes will contribute significantly to efforts to clarify the exact mechanism of BM-MNC implantation in the ischemic myocardium.

REFERENCES

1. Prockop DJ. Marrow stromal cells as stem cells for nonhematopoietic tissues. Science 1997; 276:71-74.

2. Yamashita J, Itoh H, Hirashima M, Ogawa M, Nishikawa S et al. Flk1-positive cells derived from embryonic stem cells serve as vascular progenitors. Nature 2000; 408:92-96.
3. Kamihata H, Matsubara H, Nishiue T, Fujiyama S, Tsutsumi Y et al. Implantation of bone marrow mononuclear cells into ischemic myocardium enhances collateral perfusion and regional function via side supply of angioblasts, angiogenic ligands, and cytokines. Circulation 2001; 104:1046-1052.
4. Saito T, Kuang JQ, Lin CC, and Chiu RC. Transcoronary implantation of bone marrow stromal cells ameliorates cardiac function after myocardial infarction. J Thorac Cardiovasc Surg 2003; 126:114-1123.
5. Shintani S, Murohara T, Ikeda H, Ueno T, Sasaki K et al. Augmentation of postnatal neovascularization with autologous bone marrow transplantation. Circulation 2001; 103:897-903.
6. Murohara T, Ikeda H, Duan J, Shintani S, Sasaki K et al. Transplanted cord blood-derived endothelial precursor cells augment postnatal neovascularization. J Clin Invest 2000; 105:1527-1536.
7. Strauer BE, Brehm M, Zeus T, Köstering M, Hernandez Anna et al. Repair of infarcted myocardium by autologous intracoronary mononuclear bone marrow cell transplantation in humans. Circulation 2002; 106:1913-1918.
8. Napoleone F, and Terri DS. Endocrine Reviews 1997; 18:4-25.
9. Kobayashi T, Hamano K, Li TS, Katoh T, Kobayashi S et al. Enhancement of angiogenesis by the implantation of self bone marrow cells in a rat ischemic heart model. J Surg Res 2000; 89:189-195.
10. Pelletier MP, Giaid A, Sivaraman S, Dorfman J, Li CM et al. Angiogenesis and growth factor expression in a model of transmyocardial revascularization. Ann Thorac Surg 1998; 66:12-18.
11. AsaharaT, Murohara T, Sullivan A, Silver M, van der Zee R et al. Isolation of putative progenitor endothelialcells for angiogenesis. Science 1997; 275:964-967.
12. Kawamoto A, Tkebuchava T, Yamaguchi J, Nishimura H, Yoon YS et al. Intramyocardial transplantation of autologous endothelial progenitor cells for therapeutic neovascularization of myocardial ischemia. Circulation 2003; 107:461-468.
13. Zhang S, Zhang P, Guo J, Jia Z, Ma K et al. Enhanced cytoprotection and angiogenesis by bone marrow cell transplantation may contribute to improved ischemic myocardial function. Eur J Cardiothorac Surg 2004; 25:188-195.
14. Fujioka H, Hunt PJ, Rozga J, Wu GD, Cramer DV et al. Carboxyfluorescein (CFSE) labeling of hepatocytes for short-term localization following intraportal transplantation. Cell Transplant 1994; 3:397-408.
15. Tamura R, Miyagawa J, Nishida M, Kihara S, Sasada R et al. Immunohistochemical localization of betacellulin, a member of epidermal growth factor family, in atherosclerotic plaques of human aorta. Atherosclerosis 2001; 155:413-423.
16. Iwaguro H, Yamaguchi J, Kalka C, Murasawa S, Masuda H et al. Endothelial progenitor cell vascular endothelial growth factor gene transfer for vascular regeneration. Circulation 2002; 105:732-738.
17. Krause DS, Theise ND, Collector MI, Henegariu O, Hwang S et al. Multi-organ, multi-lineage engraftment by a single bone marrow-derived stem cells. Cell 2001; 105:369-377.
18. Yoon YS, Park JS, Tkebuchava T, Luedeman C, and Losordos DW. Unexpected severe calcification after transplantation of bone marrow cells in acute myocardial infarction. Circulation 2004; 109:3154-3157.
19. Zhang S, Guo J, Zhang P, Liu Y, Jia Z et al. Long-term effects of bone marrow mononuclear cell transplantation on left ventricular function and remodeling in rats. Life Sci 2004; 74:2853-2864.
20. Sasaki K, Duan J, Murohara T, Ikeda H, Shintani S et al. Rescue of hypercholesterolemia-related impairment of angiogenesis by oral folate supplementation. J Am Coll Cardiol 2003; 42:364-372.
21. Nath R, Kumar D, Li T, and Singal PK. Metallothioneins, oxidative stress and the cardiovascular system. Toxicology 2000; 155:17-26.
22. Dai Q, Huang J, Klitzman B, Dong C, Goldschmidt-Clermont PJ et al. Engineered zinc finger-activating vascular endothelial growth factor transcription factor plasmid DNA induces therapeutic angiogenesis in rabbits with hindlimb ischemia. Circulation 2004; 110:2467-2475.

Original Contribution

Kurume Medical Journal, 54, 51-55, 2007

Perineal Hernia in Women : Assessment with Evacuation Fluoroscopic Cystocolpoproctography

YASUMI ARAKI, TOSHIHIRO NOAKE, TAKAAKI NAGAE, YUJI TOU, MOTONORI NAKAGAWA, YASUE IWATANI, HIROYUKI OZASA AND KAZUO SHIROUZU*

*Kurume Coloproctology Center, Kurume 839-0865 and *Department of Surgery, Kurume University School of Medicine, Kurume 830-0011, Japan*

Received 11 July 2007, accepted 6 November 2007

Edited by KEI MATSUOKA

Summary: The aim of this study is to assess the usefulness of fluoroscopic cystocolpoproctography in the treatment of female pelvic organ prolapse. The presence or absence of rectocele, enterocele, sigmoidocele, and the cystocele on cystocolpoproctography was retrospectively analyzed in 46 consecutive patients. A rectocele was detected in 4.5% of the patients, postvaginal hernia in 19.7%, cystocele in 3.0%, complete rectal prolapse in 53.0%, massive rectal prolapse in 10.6%, and incomplete rectal prolapse in 4.5% of the patients on cystocolpoproctography. Perineal hernia can include a combination of cystocele, rectocele, uterine prolapse, enterocele and rectal prolapse. Accurate diagnosis of the coexisting abnormalities is essential in planning reconstructive procedures so that the risks of recurrence and reoperation can be minimized. Fluoroscopic cystocolpoproctography provides direct visualization and quantification of female pelvic organ prolapse, information that usually can only be inferred by physical examination.

Key words perineal hernia, fluoroscopic cystocolpoproctography

INTRODUCTION

Hernias in the perineum can be classified as pelvic or perineal. The former includes obturator hernia and sciatic hernia, while the latter includes levator hernia, which is caused by a levator funnel in the levator ani muscles. Hernias may occur in the urogenital hiatus and anorectal hiatus. In this study, we performed fluoroscopic cystocolpoproctography to classify perineal hernias according to the system described by Amano [1] and assessed the role of this technique in the treatment of female pelvic organ prolapse.

MATERIALS AND METHODS

Forty-six women (66 lesions) who presented to our clinic with a chief complaint of perineal prolapse (or a sense of perineal prolapse) over the two-year period from January 2004 to March 2006 were the subjects of this study. Mean age was 75.7 years (21-96).

Barium was administered two hrs before examination to opacify the small bowel. Retrograde cystography with urographin was performed. A urographin-soaked gauze was inserted into the vagina and 200 mL of barium paste was injected into the rectum. Lateral images were taken at rest, during contraction and during straining with the subject sitting on a commode attached to the fluoroscopy table. As shown in Fig. 1, perineal hernias were classified on the basis of x-ray pictures taken during straining (Figs. 2, 3).

Address Correspondence to: Yasumi Araki, M.D., Kurume Coloproctology Center, 2-2-18 Shin-Aikawa, Kurume 839-0865, Japan. Tel: +81-942-43-5757 Fax: +81-942-45-2613 E-mail:Yasumi_7891@yahoo.co.jp

Abbreviation: MRI, magnetic resonance imaging.

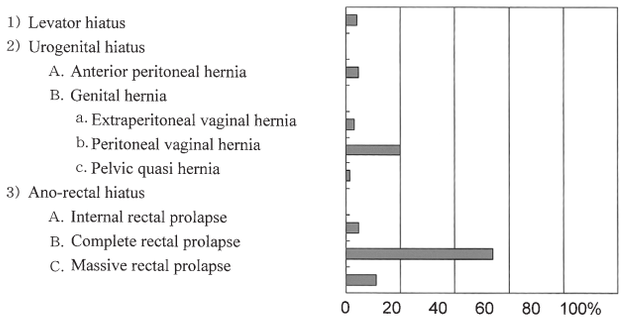

Fig. 1. Classification of perineal hernia.

Fig. 2. Cystocolpoproctography.

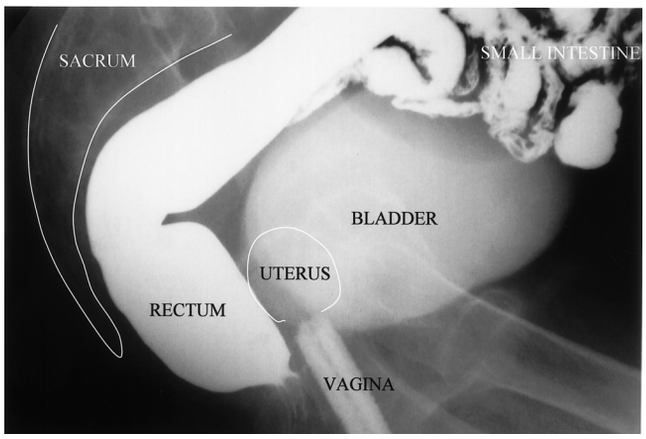

Fig. 3. Normal organ conditions.

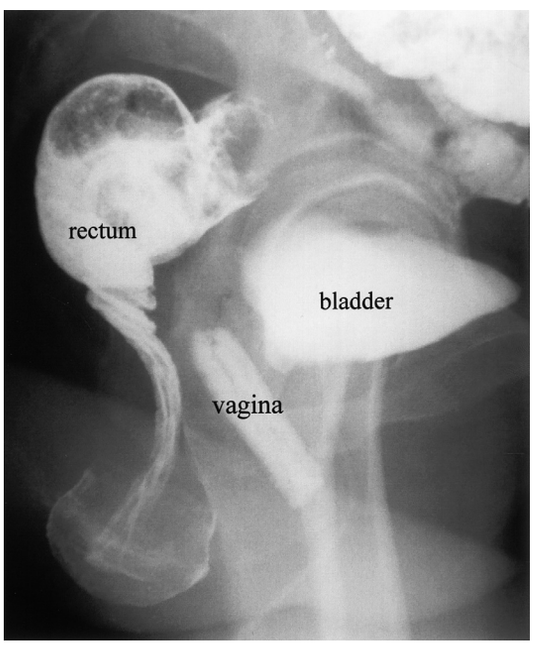

Fig. 4. Cystocolpoproctography shows the rectum is found intussuscepting and protruding form the anus as complete rectal prolapse.

RESULTS

Case 1

A 58-year-old woman visited us complaining of anal prolapse. Cystocolpoproctography showed a normal pelvic floor but the rectum was found intussuscepting and protruding from the anus (complete rectal prolapse) (Fig. 4). Rectal fixation was performed surgically.

Case 2

An 83-year-old woman visited us complaining of a sense of perineal descent. Cystocolpoproctography revealed perianal pelvic descent (levator hiatus) complicated by rectal intussusception, indicating the rectum was in a state of massive prolapse with the uterus trapped in the intussuscepting rectum (Fig. 5). Rectal fixation was performed surgically, together with levatorplasty of the anterior rectum and the Moschcowitz procedure.

Case 3

A 78-year-old woman was referred to us complaining of perineal prolapse. Cystocolpoproctography revealed posterior vaginal hernia in which the small bowel prolapsed from behind the uterus and was protruded into the vaginal wall, and massive rectal prolapse in which the small bowel was displaced into the intussuscepting rectum (Fig. 6). Rectal fixation was performed surgically, along with levatorplasty of the anterior rectum, and pelvic floor reconstruction using Composix Mesh.

Case 4

An 82-year-old woman was referred to us com-

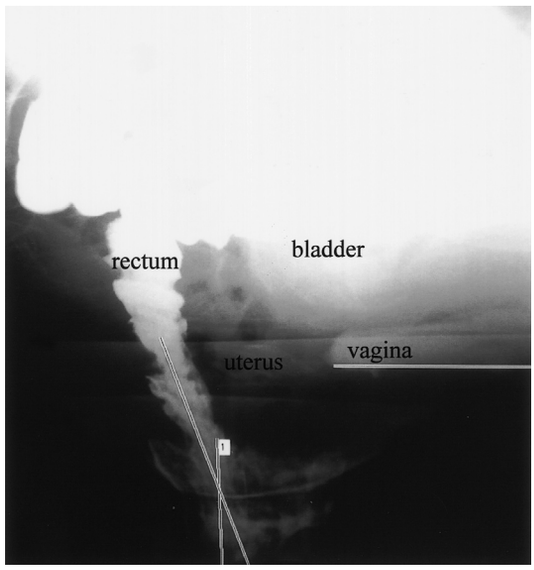

Fig. 5. Cystocolpoproctography shows the rectum is in a state of massive prolapse where the uterus is trapped in the intussuscepting rectum.

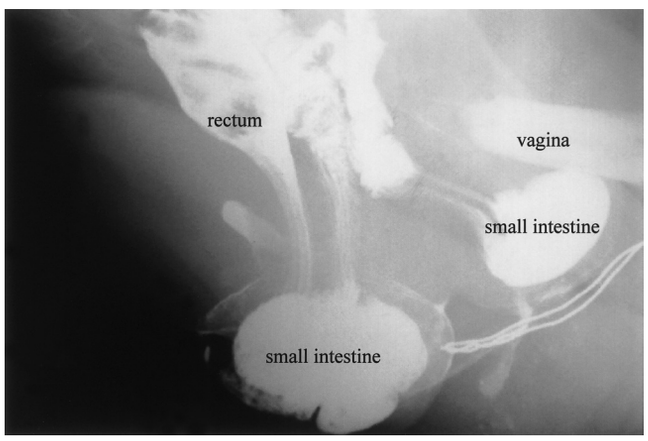

Fig. 6. Cystocolpoproctography shows posterior vaginal hernia in which the small bowel prolapsed from behind the uterus, and massive rectal prolapse in which the small bowel is displaced into the intussuscepting rectum.

plaining of a sense of perineal descent. Cystocolpoproctography revealed posterior vaginal hernia in which the sigmoid colon prolapsed from behind the uterus and was protruded into the vaginal wall (Fig. 7). Rectal fixation was performed surgically, along with pelvic floor reconstruction using Composix Mesh.

Case 5

An 85-year-old woman visited us complaining of perineal prolapse. Cystocolpoproctography revealed rectal intussusception and prolapse through the anus.

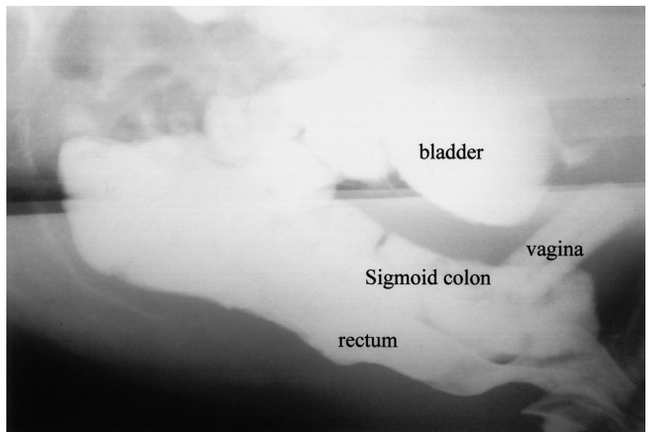

Fig. 7. Cystocolpoproctography shows posterior vaginal hernia in which the sigmoid colon prolapsed from behind the uterus and is protruded into the vaginal wall.

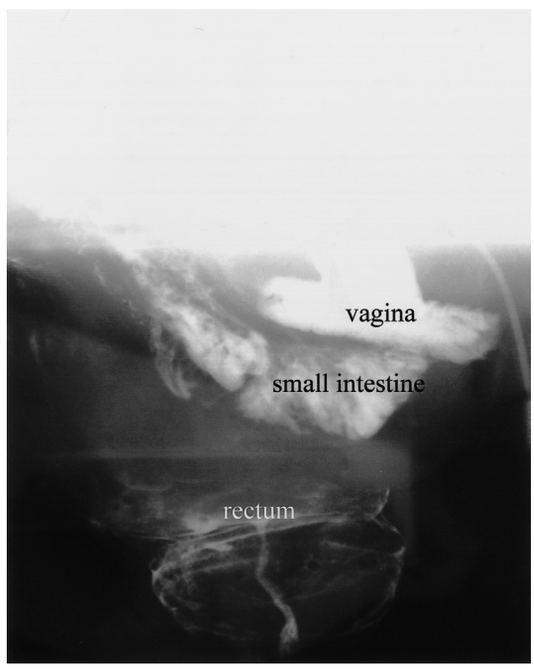

Fig. 8. Cystocolpoproctography shows rectal intussusception and prolapse through the anus as massive rectal prolapse complicated by enterocele in which the small bowel was trapped in the intussuscepting rectum.

She was diagnosed as having massive rectal prolapse complicated by enterocele in which the small bowel was trapped in the intussuscepting rectum (Fig. 8). Rectal fixation was performed surgically together with levatorplasty of anterior rectum.

Of the forty-six patients (66 lesions) who present-

ed to our clinic with a chief complaint of perineal prolapse (or a sense of perineal prolapse), 4.5% had posterior rectal sigmoidocele categorized as levator hernia, 19.7% had posterior vaginal hernia, 3.0% had cystic prolapse categorized as urogenital hiatus hernia, 53% had (simple) complete rectal prolapse, 10.6% had massive rectal prolapse and 4.5% had incomplete rectal prolapse categorized as anorectal hiatus hernia (Fig. 1).

DISCUSSION

In 1885, Thomas [2] described five types of vaginal hernia: cystocele, rectocele, vaginal enterocele, pudendal enterocele and perineal enterocele. A new classification similar to the current system was developed by Wilensky and Kaufman [3] in 1940, who categorized vaginal hernia as extravaginal hernia (including urethrocele, cystocele and rectocele), peritoneal vaginal hernia (including anterior, posterior, lateral anterior, lateral posterior and postoperative types), perineal hernia, hedrocele, pudendal hernia and pelvic quasi hernia. Hernias in the perineum can be differentiated as being either pelvic or perineal. The former includes obturator hernia and sciatic hernia. The latter is caused by levator hernia in the levator ani muscles or by hernias through the urogenital or anorectal hiatus. Hernias that pass through the urogenital hiatus include urogenital hiatus hernia, anterior peritoneal hernia and genital hernia. For genital hernia, three subtypes are recognized: extraperitoneal vaginal, peritoneal vaginal and pelvic quasi hernia. Anorectal hiatus hernia is graded relative to rectal prolapse as internal rectal prolapse where the rectum does not stick out of the anus, complete rectal prolapse where the rectum protrudes from the anus and massive rectal prolapse where the herniated rectum contains an extraperitoneal hernia. Diagnoses such as enterocele or sigmoidocele are made based on the organ that is trapped in the hernia sac.

Magnetic resonance imaging (MRI) is an easy-to-use tool that can measure the degree of descent of the intrapelvic organs. It has been reported that the rate of correct diagnosis by MRI is 66% for rectocele, 70% for cystic prolapse, 42% for uterine prolapse and 87% for enterocele [4,5]. Dynamic imaging lead to changes in the initial operative plan in 41 percent of patients and was the only modality that identified levator ani hernias. Dynamic cystocolpoproctography identified sigmoidoceles and internal rectal prolapse more often than physical examination or dynamic magnetic resonance [6].

Although it is convenient and of low invasiveness, MRI performed in the lateral decubitus position is inevitably less accurate than cystocolpoproctography performed in the sitting position with straining. The fact that it is a complicated procedure, the sense of embarrassment the patient entertains and other issues remain to be solved for cystocolpoproctography but the technique can be applied not only to morphologic investigation of the intrapelvic organs at rest, during contraction and during straining but also to cystometry and measurement of urine and stool volume over time [7].

Among our patients with perineal hernia, 4.5% had posterior rectal sigmoidocele categorized as levator hernia, 19.7% had posterior vaginal hernia, 3.0% had cystic prolapse categorized as urogenital hiatus hernia, 53.0% had (simple) complete rectal prolapse, 10.6% had massive rectal prolapse, and 4.5% had incomplete rectal prolapse categorized as anorectal hiatus hernia, while 43% of the rectal prolapse patients had complicating lesions in the pelvis. One study examined 73 patients with indefinite anal complaints by means of defecography and detected rectocele in 29%, enterocele in 18% and sigmoidocele in 5% [8]. In another series, cinedefecography demonstrated pelvic floor abnormalities in 52% of 55 women with rectal prolapse [9]. All of these studies report a similar incidence of intrapelvic complications. These findings indicate the necessity of preoperative cystocolpoproctography to examine for intrapelvic complications in rectal prolapse patients.

Extraperitoneal vaginal hernia categorized as massive rectal prolapse develops in 33% of patients who have been diagnosed from external morphology as having complete rectal prolapse. In these cases, Gant-Miwa procedure, Delorme's procedure or rectopexy used to correct rectal prolapse may have left the extraperitoneal vaginal hernia unrepaired, possibly resulting in the recurrence of hernia on the anterior rectal lining. This supports our conclusion that cystocolpoproctography is helpful not only for formulating treatment plans, but also for preventing recurrence of rectal prolapse and relieving patients' complaints.

CONCLUSION

Fluoroscopic cystocolpoproctography is the exam of choice for the functional and morphologic diagnosis of perineal hernia and plays an important role in treatment planning.

REFERENCES

1. Amano S. Posterior vaginal hernia: Report of a Case and Review of the Literature. J Jpn Soc Coloproctol 2002; 55:108-113.
2. Thomas TG. Vulvar and vaginal enterocele. NY Med J 1885; 42:705-711.
3. Wilensky AO, and Kaufman PA. Vaginal hernia. Am J Surg 1940; 49:31-41.
4. Kelvin FM, Maglinte DD, Hale DS, and Benson JT. Female pelvic organ prolapse: a comparison of triphasic dynamic MR imaging and triphasic fluoroscopic cystocolpoproctography. AJR Am J Roentgenol 2000; 174:81-88.
5. Devel B, Vulierme MP, Poilpot S, Menu Y, and Levardon M. Imaging pelvic floor prolapse. Gynecol Obstet Biol Reprod 2003; 32:22-29.
6. Kaufman HS, Buller JL, Thompson JR, Pannu HK, DeMeester SL et al. Dynamic pelvic magnetic resonance imaging and cystocolpoproctography alter surgical management of pelvic floor disorders. Dis Colon Rectum 2001; 44:1575-1583.
7. Shafik A, and Khalid AM. Fecoflowmetry in fecal incontinence. Eur Surg Res 1992; 24:61-68.
8. Kelvin FM, Maglinte DD, Hornback JA, and Benson JT. Pelvic prolapse: assessment with evacuation proctography. Radiology 1993; 186:907.
9. Peter WA, Smith MR, and Drescher CW. Rectal prolapse in women with other defects of pelvic floor support. Am J Obstet Gynecol 2001; 184:1488-1494.

Original Contribution

Kurume Medical Journal, 54, 57-63, 2007

Relationship between Radiation Pneumonitis and Prognosis in Patients with Primary Lung Cancer Treated by Radiotherapy

MOTOTSUGU YAMANO, HIROYUKI OGINO, YUTA SHIBAMOTO AND NAOTOSHI HORII*

*Department of Radiology, Nagoya City University Graduate School of Medical Sciences, Nagoya 467-8601 and *Department of Radiology, Kishiwada City Hospital, Kishiwada 596-8501, Japan*

Received 3 September 2007, accepted 7 November 2007

Edited by NAOFUMI HAYABUCHI

Summary: Relationship between the grade of radiation pneumonitis (RP) and treatment outcome in lung cancer patients has not been clarified yet. The purpose of this study was to retrospectively evaluate the relationship in patients with primary lung cancer treated by radiotherapy. One hundred thirty-five patients who underwent definitive radiotherapy with known grade of RP were analyzed. RP was scored by using the Radiation Therapy Oncology Group (RTOG) acute radiation morbidity scoring criteria. Survival and local control data were analyzed in relation to the grade of RP. RP was grade 0 in 5 patients, grade 1 in 71, grade 2 in 39, grade 3 in 15 (11%), grade 4 in 0 and grade 5 in 5 (3.7%). There were no significant correlations between patient or tumor characteristics and grade of RP. Excluding 5 patients with grade 5 pneumonitis, survival rates were similar between those with grade 0 or 1 pneumonitis and those with grade 2 or 3. Also, there was no difference in survival between patients with grade 0-2 pneumonitis and those with grade 3. Local control rates were similar between the two groups. Grade of RP did not appear to be associated with prognosis when patients with grade 5 pneumonitis were excluded from analysis.

Key words radiation pneumonitis, lung cancer, prognosis, local control

INTRODUCTION

Radiotherapy is the mainstay of treatment in patients with nonsmall cell lung cancer (NSCLC) with locally advanced disease or poor pulmonary function [1-8]. It is well documented that conventionally fractionated radiotherapy for NSCLC to a total dose of 50-60 Gy or more improves locoregional control and survival rate [9]. In addition, recent studies have shown excellent results for stage I lung cancer treated with stereotactic radiotherapy [10-12].

On the other hand, pulmonary toxicity such as radiation pneumonitis (RP) and pulmonary fibrosis commonly develops after radiation therapy. The grade of pulmonary toxicity varies in individual patients so that it may influence the prognosis of patients; severe RP was reported to be an adverse prognostic factor in patients with primary lung cancer [13]. Recently, several studies have shown that inflammatory cytokines and cell adhesion molecules play an important role in radiation-induced pulmonary injury [14]. Plasma transforming growth factor-β levels have been reported to be associated with occurrence of RP [14-16]. Also, RP is reported to be associated with levels of some interleukins and tumor necrosis factors [17,18], which have anti-tumor effects [19,20]. In our experiences, a number of patients with residual mass after radiotherapy developed severe RP, and the residual mass was cov-

Corresponding author: Hiroyuki Ogino, MD, Department of Radiology, Nagoya City University Graduate School of Medical Sciences, 1 Kawasumi, Mizuho-ku, Mizuho-cho, Nagoya 467-8601, Japan. Tel: 052-853-8276 Fax: 052-852-5244 E-mail: ogino@med.nagoya-cu.ac.jp

Abbreviations: AII, angiotensin II; ACE, angiotensin-converting enzyme; EORTC, European Organization for Research and Treatment of Cancer; MST, median survival time; NSCLC, nonsmall cell lung cancer; PS, performance status; RP, radiation pneumonitis; RTOG, Radiation Therapy Oncology Group; UICC, International Union Against Cancer; YSR, year survival rate.

ered by dense fibrosis. Thereafter, they experienced no local recurrence. Therefore, we hypothesized that severe RP may contribute to local control by developing severe inflammation around the residual tumor mass in some patients.

In this study, therefore, we attempted to investigate relationship between the grade of RP and prognosis and local control of NSCLC patients who were treated by definitive conventional radiotherapy and were followed at our hospitals; stages and RP grades could be evaluated from both clinical and radiological findings in all of these patients.

MATERIALS AND METHODS

Patients and treatment characteristics

The subjects of this study were 135 patients with histologically-confirmed NSCLC who had been appropriately staged and treated between March 1990 and August 2005, and followed until death or for at least 6 months at our hospitals. There were 112 men and 23 women. The median age of the patients was 69 years (range, 46-87 years). Patients were staged according to the 1997 International Union Against Cancer (UICC) classification system; patients seen before 1997 were restaged according to the system.

No patient underwent surgical resection. All patients were treated using 4, 6 or 10 MV photons from linear accelerators. The patients were generally treated with 1.8-2.0 Gy daily fractions using parallel opposed anteroposterior fields to 40-45 Gy, followed by off-cord oblique fields to 58-75.2 Gy (median, 66 Gy). Patients receiving a total dose of 57 Gy or less were excluded. Sixty-five patients received variable systemic platinum-based chemotherapy.

Evaluation of RP

RP was scored according to the Radiation Therapy Oncology Group (RTOG) and the European Organization for Research and Treatment of Cancer (EORTC) acute radiation morbidity scoring criteria (Table 1) [21].

Statistical analysis

Differences in distribution of patient, tumor and treatment characteristics and rates of local relapse between lower-grade RP and higher-grade RP groups were examined by the Mantel-Haenszel χ^2 test. Overall survival rates of the patients were calculated from the date of starting radiotherapy using the Kaplan-Meier method, and differences between the curves were examined by the log-rank test. Differences were considered significant when a P value was <0.05. Multivariate analysis of potential prognostic factors was carried out using the Cox proportional hazards model. All analyses were performed using a computer software StatView version 5 (SAS Institute Inc., Cary, NC, USA).

TABLE 1.
Criteria for scoring radiation pneumonitis (RTOG/EORTC)

Grade	Signs and symptoms
0	None
1	Mild symptoms; dry cough or dyspnea on exertion Slight radiographic appearances
2	Persistent cough requiring narcotic antitussive agent/ dyspnea with minimal effort but not at rest Patchy radiographic appearances
3	Severe cough unresponsive to narcotic antitussive or dyspnea at rest/intermittent oxygen may be required Dense radiographic changes
4	Severe respiratory insufficiency/continuous oxygen or assisted ventilation required
5	Death directly related to radiation toxicity

RESULTS

There were 99 deaths during follow-up. Causes of death were cancer in 72 patients, RP-related in 5, and other in 4 patients (traffic accident, emphysema, bacterial pneumonia, and suicide in 1 patient each). The cause of death was unknown in the remaining 18 patients. For all 135 patients, median survival time (MST) was 15 months and overall survival rates were 62%, 21%, and 15% at 1, 3, and 5 years, respectively. The 5-year overall survival rate was 13% for stage I patients, 23% for stage Ⅱ, 14% for stage ⅢA and 10% for stage ⅢB.

Of the 135 patients, RP was grade 0 in 5 (3.7%), grade 1 in 71 (53%), grade 2 in 39 (29%), grade 3 in 15 (11%), grade 4 in none (0%) and grade 5 in 5 (3.7%). Relationship between RP grades and patient and tumor characteristics including age, gender, World Health Organization performance status (PS), clinical stage, primary tumor location (upper lobe vs. middle or lower lobe) and tumor histology, total radiation dose, use of chemotherapy, and local control are shown in Tables 2 and 3. There were no differences in any of these characteristics when lower-grade RP groups (grade 0, 1 or 0-2) were compared with higher-grade RP groups (grade 2-5 or 3-5). Also, these tables showed that there were no unbalances in distribution of these

factors between lower-grade RP groups (grade 0, 1 or 0-2) and higher-grade RP groups (grade 2, 3 or 3) for comparison of their prognoses.

Figure 1 shows survival curves for the 130 patients, excluding 5 patients with grade 5 RP, according to the grade of RP (grade 0 or 1 vs. grade 2 or 3). There was no difference in prognosis of the patients. Figure 2 shows survival curves for patients with grade 0-2 RP and those with grade 3 RP; again, there was no difference in prognosis of the patients (P=0.10). Figure 3 shows survival curves for stage Ⅲ patients with grade 0-2 RP and those with grade 3 RP, and there was no difference in prognosis of the patients (P=0.33).

Table 4 summarizes MST and 3-year survival rate (3-YSR) according to 9 potential prognostic factors (age, gender, PS, stage, tumor location, histology, total radiation dose, use of chemotherapy, and RP grade), excluding 5 patients with grade 5 RP. Patients with upper lobe tumors had better survival than those with middle or lower lobe tumors, and stage Ⅰ or Ⅱ patients tended to do better than stage Ⅲ patients (P=0.060). Patients receiving higher doses (above median: >66 Gy) had better survival than those receiving lower doses. Multivariate analysis was carried out for 4 factors with $P \leq 0.1$ (stage, tumor location, radiation dose and RP grade); clinical stage and radiation dose were found to have significant influences on patient survival, whereas tumor location and RP grade were not. Figure 4 shows overall survival curves according to the total radiation dose, including 5 patients with grade 5 RP. In this analysis too, patients receiving higher doses did better than those receiving lower doses.

Local control status was known in 110 patients excluding 5 patients with grade 5 RP. We could not determine the exact date of local recurrence in many patients, so Kaplan-Meier analysis was not possible. Local relapse was observed in 34 of 67 patients (51%) with grade 0 or 1 RP, while it was seen in 20 of 43 patients (47%) with grade 2 or 3 RP (P=0.61). Also, local relapse was seen in 52 of 101 patients (51%) with grade 0-2 RP and in only 2 of 9 patients (22%) with grade 3 RP; the difference was, however, not sig-

TABLE 2.
Patient and tumor characteristics versus grades of radiation pneumonitis

	Grade 0-2	Grade 3-5	*P*	Grade 3	*P*
Age (years)					
Mean±SD	68±9	71±8	0.24	69±6	0.82
<70	58	9	0.82	8	0.83
≥70	57	11		7	
Gender					
Male	95	17	1.0	12	0.80
Female	20	3		3	
PS					
0, 1	92	16	1.0	11	1.00
2, 3, 4	23	4		4	
Clinical stage					
Ⅰ, Ⅱ	21	6	0.36	5	0.36
Ⅲ	94	14		10	
Tumor location					
Upper lobe	77	13	1.0	9	0.81
Middle or lower lobe	38	7		6	
Histological diagnosis					
Squamous cell	63	10	0.88	6	0.42
Adeno or large cell	52	10		9	
Total radiation dose (Gy)					
≤66	64	11	0.95	8	1.0
>66	51	9		7	
Chemotherapy					
Yes	57	8	0.58	8	0.14
No	58	12		7	
Local control					
Yes	52	2	0.16	2	0.16
No	49	7		7	

No patients had grade 4 RP.

TABLE 3.
Patient and tumor characteristics versus grades of radiation pneumonitis

	Grade 0, 1	Grade 2-5	*P*	Grade 2, 3	*P*
Age (years)					
Mean±SD	69±9	68±9	0.50	67±9	0.23
<70	36	31	0.67	30	0.48
≥70	40	28		24	
Gender					
Male	59	53	0.10	48	0.14
Female	17	6		6	
PS					
0, 1	57	51	0.15	46	0.24
2, 3, 4	19	8		8	
Clinical stage					
I, II	17	10	0.57	9	0.26
III	59	49		45	
Tumor location					
Upper lobe	50	40	0.95	36	0.92
Middle or lower lobe	26	19		18	
Histological diagnosis					
Squamous cell	42	31	0.89	27	0.68
Adeno or large cell	34	28		27	
Total radiation dose (Gy)					
≤66	40	35	0.44	32	0.45
>66	36	24		22	
Chemotherapy					
Yes	34	31	0.47	31	0.15
No	42	28		23	
Local control					
Yes	34	20	0.61	20	0.61
No	33	23		23	

No patients had grade 4 RP.

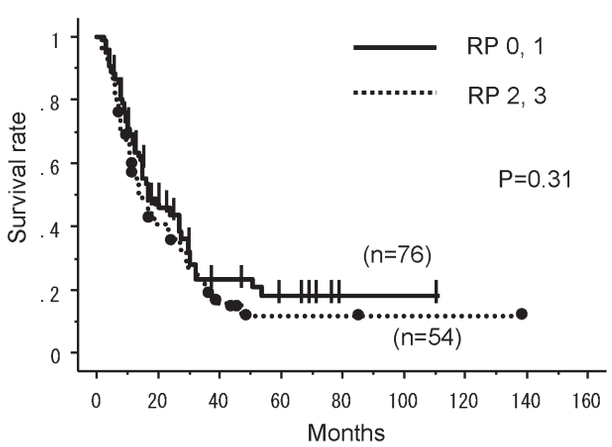

Fig. 1. Overall survival curves according to the grade of RP (grade 0, 1 vs 2, 3). There was no significant difference in survival between the two groups (*P*=0.31).

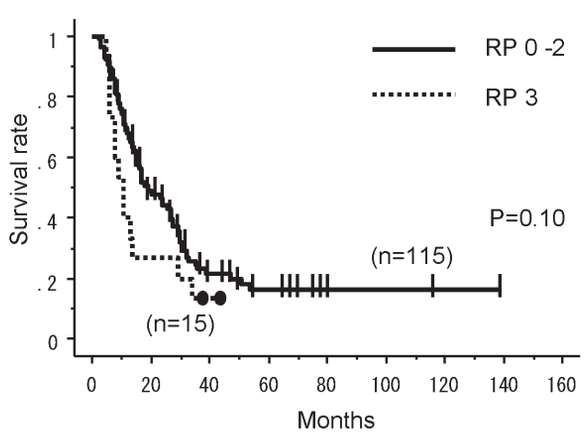

Fig. 2. Overall survival curves according to the grade of RP (grade 0-2 vs 3). The difference between the two groups was not significant (*P*=0.10).

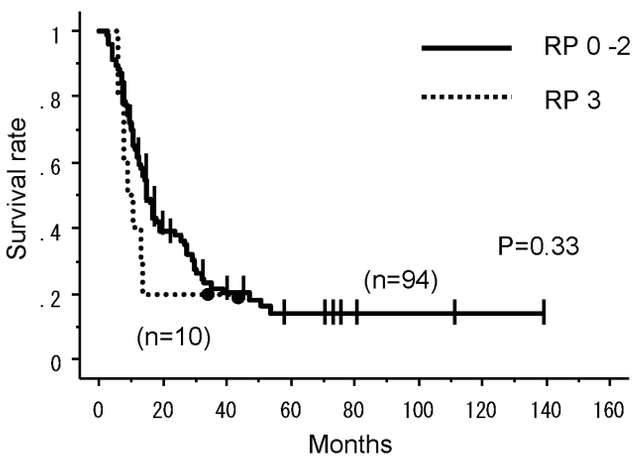

Fig. 3. Overall survival curves for stage Ⅲ patients according to the grade of RP (grade 0-2 vs 3). The difference between the two groups was not significant (*P*=0.33).

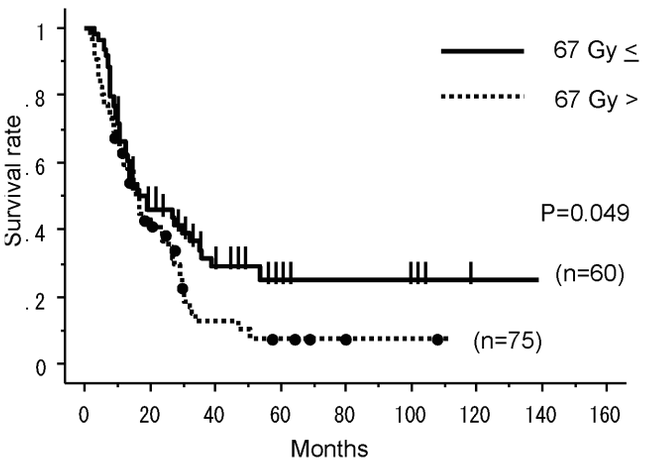

Fig. 4. Overall survival curves according to the total radiation dose. The difference between the two groups was significant (*P*=0.049).

TABLE 4.
Median survival time and 3-year survival rate according to potential prognostic factors

	n	MST (months)	3-YSR (%)	*P* (Univariate)	*P* (Multivariate)
Age (years)					
<70	67	14.5	23	0.35	—
≥70	63	17	20		
Gender					
Male	107	18	21	0.75	—
Female	23	13.5	23		
PS					
0, 1	103	24	24	0.13	—
2-4	27	11	13		
Clinical stage					
Ⅰ, Ⅱ	27	24.5	19	0.060	0.034
Ⅲ	103	13	22		
Primary tumor location					
Upper lobe	86	16	26	0.048	0.13
Middle or lower lobe	44	12	14		
Histological diagnosis					
Squamous cell	69	12.5	19	0.16	—
Adeno or large cell	61	16.5	26		
Total radiation dose (Gy)					
≤66	72	15	14	0.049	0.024
>66	58	15.5	33		
Chemotherapy					
Yes	65	16.5	19	0.53	—
No	65	13.5	25		
RP grade					
0-2	115	16	23	0.10	0.083
3	15	9	13		

No patients had grade 4 RP. Five patients with grade 5 RP were excluded.

nificant (P=0.16).

Five patients with grade 5 RP had received radiation doses of 60, 60, 66, 70, and 72 Gy, respectively. Their survival time was only 2, 2, 3.5, 4, and 2.5 months, respectively. Although no local tumor regrowth was noted in any of the patients at the time of their death, observation period was considered to be too short to evaluate local control in these patients.

DISCUSSION

We analyzed treatment outcome in 135 patients with stage I-Ⅲ NSCLC treated by definitive radiotherapy. The 5-year overall survival rate was 15%, which is not better than previously reported results [3-5]. This may not be surprising because 80% of the patients had stage Ⅲ disease. The overall survival rates for stage I patients (13% at 5 years) were apparently low as compared with the recently reported results of stereotactic radiotherapy [10-12]. This low survival rate was partly due to a relatively large number of intercurrent death in stage I patients, seen in 8 of 13 patients. Nevertheless, it seems clear that the results of stereotactic irradiation for stage I patients are far better than those for conventional radiotherapy.

RP is one of the most common and important complications in patients with lung cancer who undergo radiation therapy to the thorax. The incidence of severe RP ranges from approximately 5% to 15% with radiotherapy or chemoradiotherapy [22-24]. In the present study, 15% of the patients had grade 3 or higher RP, and 5 (3.7%) died of severe RP. The incidence of grade 3-5 RP in the present study is not remarkably different from those reported previously, although the incidence of grade 5 RP appears slightly higher [13,25].

In several studies, age, gender, PS, clinical stage, primary tumor location (upper lobe vs. middle or lower lobe), tumor histology, and use of chemotherapy have been reported to be associated with the incidence of severe RP [26-29]. However, no significant relationship was observed in the present study between the grade of RP and patient, tumor or treatment characteristics. Analysis of larger numbers of patients may prove subtle differences regarding association of these factors with the severity of RP. Radiation field size could not be evaluated, but RP grade distribution was not correlated with tumor stage.

We found no significant difference in survival between patients with grade 0 or 1 RP and those with grade 2 or 3 RP. Also, no significant difference was found between patients with grade 0-2 RP and those with grade 3 RP. This was also true when only stage Ⅲ patients were analyzed. These results are in contrast to those reported by Inoue et al. [13] who showed that severe RP (RTOG grade 3 or 4) was associated with worse prognosis. In our experiences, severe RP, whenever it recovers, does not seem to adversely affect the patient prognosis. However, our hypothesis that severe but recoverable RP might contribute to improved prognosis was not supported. On the other hand, only 2 of 9 patients with grade 3 RP developed local recurrence. In future, further analysis with respect to local tumor control with larger numbers of patients, preferably in a prospective fashion, may more clearly answer our question.

If high-grade inflammation associated with severe RP does not contribute to improved tumor control, strategies to prevent RP should be of clinical importance. Recently, it has been shown that protective effect of angiotensin-converting enzyme (ACE) inhibitors and angiotensin Ⅱ (AⅡ) type 1 receptor blocker from RP is a topic of considerable interest [14,23]. Several groups reported that ACE inhibitors especially captopril and AⅡ type 1 receptor blocker were effective in protecting lungs from RP and the development of lung fibrosis in rat radiation injury [30-32]. The possibility remains that administration of ACE inhibitors and AⅡ type 1 receptor blocker might have two beneficial effects: control of radiation-induced side effects and control of hypertension in the future.

CONCLUSION

High-grade RP did not appear to affect prognosis of patients with NSCLC undergoing definitive radiotherapy. However, further prospective studies with larger number of patients appear to be warranted to draw a definite conclusion.

REFERENCES

1. Simpson JR, Bauer M, Perez CA, Wasserman TH, Emami B et al. Radiation therapy alone or combined with misonidazole in the treatment of locally advanced non-oat cell lung cancer: report of an RTOG prospective randomized trial. Int J Radiat Oncol Biol Phys 1989; 16:1483-1491.
2. Perez CA, Stanley K, Rubin P, Kramer S, Brady L et al. A prospective randomized study of various irradiation doses and fractionation schedules in the treatment of inoperable non-oat-cell carcinoma of the lung. Preliminary report by the Radiation Therapy Oncology Group. Cancer 1980; 45:2744-2753.
3. Schild SE, Wong WW, Vora SA, Halyard MY, Northfelt DW et al. The long-term results of a pilot study of three times a day radiotherapy and escalating doses of daily cis-

platin for locally advanced non-small-cell lung cancer. Int J Radiat Oncol Biol Phys 2005; 62:1432-1437.
4. Kubota K, Furuse K, Kawahara M, Kodama N, Yamamoto M et al. Role of radiotherapy in combined modality treatment of locally advanced non-small-cell lung cancer. J Clin Oncol 1994; 12:1547-1552.
5. Hayakawa K, Mitsuhashi N, Nakajima N, Saito Y, Mitomo O et al. Radiation therapy for Stage I-Ⅲ epidermoid carcinoma of the lung. Lung Cancer 1992; 8:213-224.
6. Alberg AJ, Brock MV, and Samet JM. Epidemiology of lung cancer: looking to the future. J Clin Oncol 2005; 23:3175-3185.
7. Nakaya N, Goto K, Saito-Nakaya K, Inagaki M, Otani T et al. The lung cancer database project at the National Cancer Center, Japan: study design, corresponding rate and profiles of cohort. Jpn J Clin Oncol 2006; 36:280-284.
8. Yamada K, Iwai K, Kawamorita R, Okuno Y, and Nakajima T. Change in Dose Distribution of Three-dimensional Conformal Radiotherapy during Treatment for Lung Tumor. Radiat Med 2006; 24:122-127.
9. Clinical practice guidelines for the treatment of unresectable non-small-cell lung cancer. J Clin Oncol 1997; 15:2996-3018.
10. Uematsu M, Shioda A, Tahara K, Fukui T, Yamamoto F et al. Focal, high dose, and fractionated modified stereotactic radiation therapy for lung carcinoma patients: a preliminary experience. Cancer 1998; 82:1062-1070.
11. Uematsu M, Shioda A, Suda A, Fukui T, Ozeki Y et al. Computed tomography-guided frameless stereotactic radiotherapy for stage I non-small cell lung cancer: a 5-year experience. Int J Radiat Oncol Biol Phys 2001; 51:666-670.
12. Onishi H, Araki T, Shirato H, Nagata Y, Hiraoka M et al. Stereotactic hypofractionated high-dose irradiation for stage I nonsmall cell lung carcinoma: clinical outcomes in 245 subjects in a Japanese multiinstitutional study. Cancer 2004; 101:1623-1631.
13. Inoue A, Kunitoh H, Sekine I, Sumi M, Tokuuye K et al. Radiation pneumonitis in lung cancer patients: a retrospective study of risk factors and the long-term prognosis. Int J Radiat Oncol Biol Phys 2001; 49:649-655.
14. Tsoutsou PG, and Koukourakis MI. Radiation pneumonitis and fibrosis: mechanisms underlying its pathogenesis and implications for future research. Int J Radiat Oncol Biol Phys 2006; 66:1281-1293.
15. Anscher MS, Marks LB, Shafman TD, Clough R, Huang H et al. Using plasma transforming growth factor beta-1 during radiotherapy to select patients for dose escalation. J Clin Oncol 2001; 19:3758-3765.
16. Bentzen SM. Preventing or reducing late side effects of radiation therapy: radiobiology meets molecular pathology. Nat Rev Cancer 2006; 6:702-713.
17. Chiang CS, Liu WC, Jung SM, Chen FH, Wu CR et al. Compartmental responses after thoracic irradiation of mice: strain differences. Int J Radiat Oncol Biol Phys 2005; 62:862-871.
18. Chen Y, Hyrien O, Williams J, Okunieff P, Smudzin T et al. Interleukin (IL)-1A and IL-6: applications to the predictive diagnostic testing of radiation pneumonitis. Int J Radiat Oncol Biol Phys 2005; 62:260-266.
19. Nakamoto T, Inagawa H, Takagi K, and Soma G. A new method of antitumor therapy with a high dose of TNF perfusion for unresectable liver tumors. Anticancer Res 2000; 20:4087-4096.
20. Parmiani G, Rivoltini L, Andreola G, and Carrabba M. Cytokines in cancer therapy. Immunol Lett 2000; 74:41-44.
21. Cox JD, Stetz J, and Pajak TF. Toxicity criteria of the Radiation Therapy Oncology Group (RTOG) and the European Organization for Research and Treatment of Cancer (EORTC). Int J Radiat Oncol Biol Phys 1995; 31:1341-1346.
22. Roach Ⅲ M, Gandara DR, Yuo HS, Swift PS, Kroll S et al. Radiation pneumonitis following combined modality therapy for lung cancer: analysis of prognostic factors. J Clin Oncol 1995; 13:2606-2612.
23. Mehta V. Radiation pneumonitis and pulmonary fibrosis in non-small-cell lung cancer: pulmonary function, prediction, and prevention. Int J Radiat Oncol Biol Phys 2005; 63:5-24.
24. Schallenkamp JM, Miller RC, Brinkmann DH, Foote T, and Garces YI. Incidence of radiation pneumonitis after thoracic irradiation: Dose-volume correlates. Int J Radiat Oncol Biol Phys 2007; 67:410-416.
25. Wang JY, Chen KY, Wang JT, Chen JH, Lin JW et al. Outcome and prognostic factors for patients with non-small-cell lung cancer and severe radiation pneumonitis. Int J Radiat Oncol Biol Phys 2002; 54:735-741.
26. Monson JM, Stark P, Reilly JJ, Sugarbaker DJ, Strauss GM et al. Clinical radiation pneumonitis and radiographic changes after thoracic radiation therapy for lung carcinoma. Cancer 1998; 82:842-850.
27. Hope AJ, Lindsay PE, Naqa IE, Alaly JR, Vicic M et al. Modeling radiation pneumonitis risk with clinical, dosimetric, and spatial parameters. Int J Radiat Oncol Biol Phys 2006; 65:112-124.
28. Segawa Y, Takigawa N, Kataoka M, Takata I, Fujimoto N et al. Risk factors for development of radiation pneumonitis following radiation therapy with or without chemotherapy for lung cancer. Int J Radiat Oncol Biol Phys 1997; 39:91-98.
29. Mah K, Keane TJ, Dyk JV, Braban LE, Poon PY et al. Quantitative effect of combined chemotherapy and fractionated radiotherapy on the incidence of radiation-induced lung damage: a prospective clinical study. Int J Radiat Oncol Biol Phys 1994; 28:563-574.
30. Molteni A, Moulder JE, Cohen EF, Ward WF, Fish BL et al. Control of radiation-induced pneumopathy and lung fibrosis by angiotensin-converting enzyme inhibitors and an angiotensin Ⅱ type 1 receptor blocker. Int J Radiat Biol 2000; 76:523-532.
31. Wang LW, Fu XL, Clough R, Sibley G, Fan M et al. Can angiotensin-converting enzyme inhibitors protect against symptomatic radiation pneumonitis? Radiat Res 2000; 153:405-410.
32. Ward WF, Lin PJP, Wong PS, Behnia R, and Jalali N. Radiation pneumonitis in rats and its modification by the angiotensin-converting enzyme inhibitor captopril evaluated by high-resolution computed tomography. Radiat Res 1993; 135:81-87.

Original Contribution

Kurume Medical Journal, 54, 65-72, 2007

A Life Span Study of Exploratory Eye Movements in Healthy Subjects: Gender Differences and Affective Influences

SACHIKO NISHIURA, YOUKO NAKASHIMA*, KEIICHIRO MORI, TAKAYUKI KODAMA*, SATOSHI HIRAI*, TAKATSUGU KURAKAKE* CHIYOMI EGAMI** AND KIICHIRO MORITA*

*Department of Neuropsychiatry, Kurume University School of Medicine, *Cognitive and Molecular Research Institute of Brain Diseases and ** Department of Pediatrics and Child Health, Kurume University School of Medicine, Kurume 830-0011, Japan*

Received 18 April 2007, accepted 30 November 2007

Edited by RYOJI YAMAKAWA

Summary: To evaluate age and gender differences as well as effects of affection, we examined exploratory eye movements. Exploratory eye movements were recorded in healthy subjects (57 women and 57 men) ranging from 9 to 74 years. All subjects were divided into three groups as pre puberty, young, and older adults to study the influences of age and gonadal hormones. Exploratory eye movements were analyzed for total eye scanning length (TESL), and total numbers of gaze points (TNGP) as subjects viewed neutral or affectively charged pictures. TESL and TNGP in older adults were significantly larger than that in both pre puberty and young adults for crying babies. TESL and TNGP in pre puberty were significantly smaller than that in both young and older adults for circles. TESL and TNGP in pre puberty were significantly smaller than that in older adults for smiling babies. Pre puberty and young adult of both genders for crying babies showed significantly shorter TESL than for when smiling babies. When viewing circles, young adult women had shorter TESL than men. TNGP in young adult women was smaller than in men for circles or crying babies. TNGP of young adult women in the visual right field was significantly smaller than in men. TNGP for crying babies was significantly smaller than that for smiling babies in young adults of both genders for the left field. Exploratory eye movements thus are a useful marker of visual cognitive function. Gender differences were limited to younger adults, suggesting influences of gonadal hormones.

Key words exploratory eye movements, gender difference, affective stimuli, laterality, visual cognition

INTRODUCTION

Eye movements have attracted attention as biologic markers. For example, patients with psychiatric disorders such as schizophrenia or affection have been compared with healthy subjects [1-3]. Holzman et al. [1] reported that schizophrenic patients have less global accuracy smooth pursuit and lower pursuit gain than normal control subjects.

In studies of exploratory eye movements, subjects are examined with an eye-mark recorder as they view several pictures while the points of gaze are analyzed in terms of several elements [3]. This assessment method, considered to reflect abnormalities of eye movements and visual information processing in natural settings, is a useful psycho-physiological marker of visual cognitive function that first requires extensive evaluation in healthy controls, concerning age and gender differences [4,5]. The authors suggested that exploratory eye movements in young adult women have been demonstrated to have a more limited eye movement range, with longer maintenance of gaze in

Corresponding author: Kiichiro Morita, Cognitive and Molecular Research Institute of Brain Diseases, Kurume University, 67 Asahi-machi, Kurume 830-0011, Japan. Tel: 0942-31-7581 Fax: 0942-31-7911 E-mail: kiichiro@med.kurume-u.ac.jp

Abbreviations: TESL, total eye scanning length; TNGP, total numbers of gaze points.

a given direction, than men of similar age, suggesting a possible gonadal hormonal influences [4,5]. One reason why such analyses are important involves, reported gender differences in aspects of brain function. Men have been found perform better than women in certain spatial, motor [6-8], and language tasks [9] as well as in scanning the visual field [10]. Gender differences in event related potentials (ERPs) concerning visual information processing have been reported [11-13] and also might involve gonadal hormones [6,14,15].

Affect and the following emotion are basically important between human relationships in human life events. Because, a negative affection as cry, fear should obstruct life events, however, a positive affection as pleasure, happy should facilitate of life behavior. The effects of affective stimuli have been reported in event-related potentials, especially P300 components [13,16]. Those authors reported the P300 amplitude was larger for the negative affection as angry or sad than that for the positive affection as pleasure or neutral stimuli and suggested that event-related potentials was useful biological marker to evaluate the effects of affection. Thus, it is important to study the effects of affections on the cognitive function for exploratory eye movements as one of the biological marker. Indeed, the exploratory eye movement was inhibited in depressive patients [17], because of depressive emotion.

The present study was performed to examine whether gender differences of exploratory eye movements were observed or not, during the three life phases as the pre puberty (children), puberty (young adult) and post puberty (elder adults) of the healthy, and the affective stimuli (smiling and crying babies). The second aim of the present study was, whether or not there is any gender and/or age difference for affective stimulus.

MATERIALS AND METHODS

Subjects

A group of 114 healthy paid volunteers (9 to 74 years) (mean age ± SD, 35.9±19.3 years). All subjects were divided into three groups as pre puberty (12 boys and 12 girls: 10.2±0.9 and 10.5±1.4, respectively), young adults (27 men and 27 women: 30.5±6.5 and 30.3±7.2, respectively), and older adults (post puberty) (18 men and 18 women: 59.5±6.3 and 60.9±8.6, respectively). No significant age differences were observed in each life phase. Women were not recorded at any particular time during the menstrual periods. All subjects were right handed, had normal vision, and had no history of psychiatric or neurological diseases or drug addiction. All subjects gave written informed consent for study participation. The ethics Committee of Kurume University approved the present study.

Eye mark recording

Eye movements were recorded using an eye mark recorder (Nac, EMR-8, Tokyo, Japan) that consisted of two video cameras (left- and right-eye mark-shooting units) fixed to the left and right sides of a headband and another camera (field-shooting unit) fixed to the top of a helmet. Infrared light (850 nM) sources were positioned in front of each lower eyelid. The side cameras recorded the infrared light reflected from the cornea of the eye. The camera on the top of the cap recorded the pictures shown on the screen. After a camera controller superimposed these three recordings with a 0.01 sec electronic timer, the combined recording was saved on videotape. Movement of more than 1° with duration greater than 0.1 sec was scored as an eye movement. Accordingly, the gazing point was determined from a gazing time exceeding 0.1 sec. This technique enabled us to determine eye fixation points. Recorded data were assessed by a computer analysis system. In the present study, exploratory eye movements were analyzed for two parameters: total eye scanning length (TESL) for gazing points, total number of gazing points (TNGP) as reported before [2,4]. Furthermore, in the present study, we divided the measures as TNGP to the right half and the left half field of the screen as the total number of gazing points of the left field (TNGP-l) and the right field (TNGP-r) of screen, and counted the total number of transferring between the left and the right fields. Eye scanning length was calculated from the distance between two eye gazing points as reported previously [2,4].

Eye movement recording procedure

In a darkened room where visual and auditoria sensory stimuli were attenuated, eye movement was recorded using the eye-mark recorder. Before eye movements were recorded, subjects were instructed to confirm each subsequently viewed picture exactly as presented. All subjects were also instructed to view and fix several corners' points to check their eye movements to evaluate neurological deficits and low-level eye movement as reflex organic saccade. All subjects have no deficits in the present procedure. Exploratory eye movements and fixation points during perception of pictures were examined. The pictures were project-

ed onto a screen to form images 120 cm wide and 90 cm tall. Maximum angles of sight lines were 40° horizontally and 24° vertically. Each block consisted of a series of three pictures each presented for 15 sec.

Three kinds of pictures were used as shown in Fig. 1. The picture of steps on: two symmetrical smiling babies with smiling sound (70 dB, SPL) examining possible emotional influences. Picture of steps at center: Two symmetrical crying babies with crying sound (70 dB, SPL) examining possible emotional influences. The picture of steps below: two symmetrical simple circles to examine drive and motivation in subjects.

The crying babies and the smiling babies were counterbalanced. The recording was done as follows. At session 1: all subjects were asked, "Look the front pictures freely." (free condition). At session 2: all subjects were asked "Look the front picture carefully and memorize" because "I will ask you immediately after recording, what picture did you see?" (memorized condition). At session 3: all subjects were asked, "Are there any differences between the present picture and the former one? " to test confidence and attention (confidence condition). Data were analyzed from the right eye and the left eye in the present study. There was no significant difference of analyzing elements in the eye movements between the right and left eyes.

Statistical analysis

In the present study, we used the data only obtained from the confidence condition (session 3), because the confidence condition was mostly reflecting the visual cognitive function [2]. For data, one-way repeated analysis of variance (ANOVA) was performed to determine epsilon factors using G to G and H to F epsilon. A two-way (gender × stimuli or gender × field) ANOVA was used to compute the main gender and the main stimuli and the field effects in each life period (childhood, young adulthood and older adulthood). Whether interaction was obtained or not, one-way ANOVA was used. A one-way ANOVA (gender, stimulus, field) was used to compute the main gender, group, stimulus and field effects Post-hoc analyses were conducted using Scheffe tests. A level of $p<0.05$ was accepted as statistically significant.

RESULTS

Typical sequences of the exploratory eye movements for one healthy adult men and women viewing three pictures are shown in Fig. 1. The subject showed

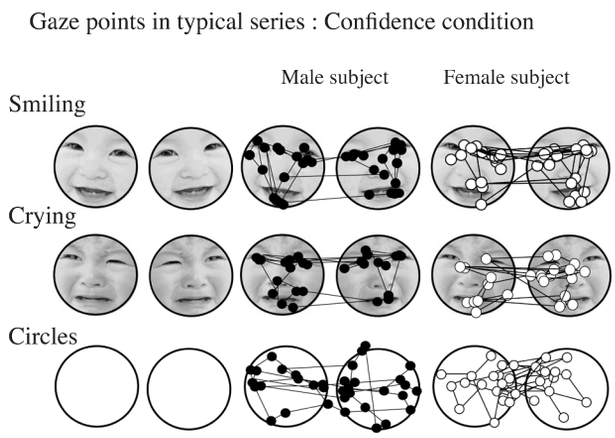

Fig. 1. Three pictures used (left) and typical series of exploratory eye movements in a young adult man (middle) and woman (right). Each dot indicates a gaze point and each line, a movement. The gaze points were located centrally in simple circles, especially in woman.

TABLE 1.
Exploratory eye movements in confidence condition

		Pre-puberty	Young adult	Older adult
TESL (cm) Female	Smiling	518.2±164.7	566.0±156.7	607.0±107.0
	Crying	422.5±162.7	452.7±153.7	560.0±167.5
	Circles	424.0±144.1	458.3±132.6	556.3±164.3
Male	Smiling	534.7±167.6	592.2±116.7	603.7±114.7
	Crying	430.5±153.4	474.2±161.2	536.9±157.8
	Circles	417.0±120.8	569.4±134.0	567.4±198.3
TNGP (n) Female	Smiling	26.6±3.4	27.8±5.2	29.3±4.7
	Crying	25.4±3.8	23.6±5.6	27.0±5.7
	Circles	23.5±2.5	24.6±5.6	27.1±6.8
Male	Smiling	27.1±5.1	28.8±5.3	28.6±3.7
	Crying	23.4±3.4	26.3±6.9	27.3±4.3
	Circles	24.3±5.1	28.9±5.0	26.5±4.8

TESL, total eye scanning length; TNGP, total number of gaze points.

clear eye movements, which attached to left and right baby's eyes and mouth. The gazing points tended to expand in pictures, smiling and circles but not in crying pictures (Fig. 1, Table 1).

Total eye scanning length (TESL) (Figs 2, 3)

Pre puberty: The main gender difference by two-way ANOVA (gender × stimuli) was not significant, but the main stimulus difference was significant [F=6.9, p<0.01]. There was no interaction observed between gender and stimuli. The TESL when viewing smiling babies was significantly longer than that of both the crying babies (p<0.01) and the circles (p<0.01). There were no gender differences observed by one-way ANOVA (gender). In girls, TESL [F=3.0, p<0.05] when viewing crying babies was significantly shorter (p<0.05) than those in smiling babies. In boys, TESL [F=4.3, p<0.05] when viewing crying babies was significantly shorter than those in smiling babies (p<0.05) and the circles (p<0.05).

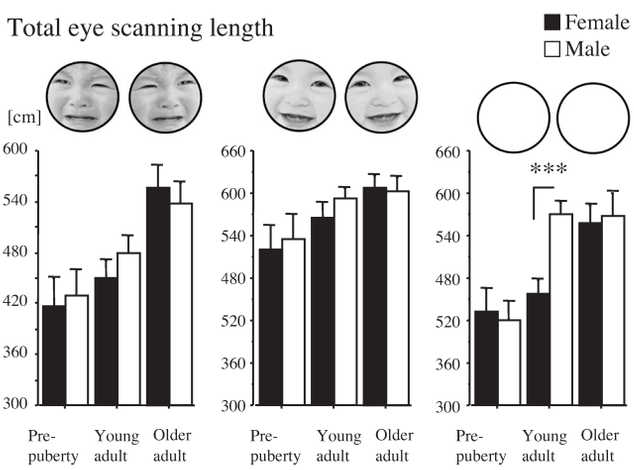

Fig. 2. Total eye scanning length (TESL; ordinate) was plotted against groups and stimuli (abscissa). TESL was clearly prolonged when men viewed the circles. Asterisks indicate significant differences between women and the men. ***: p<0.001

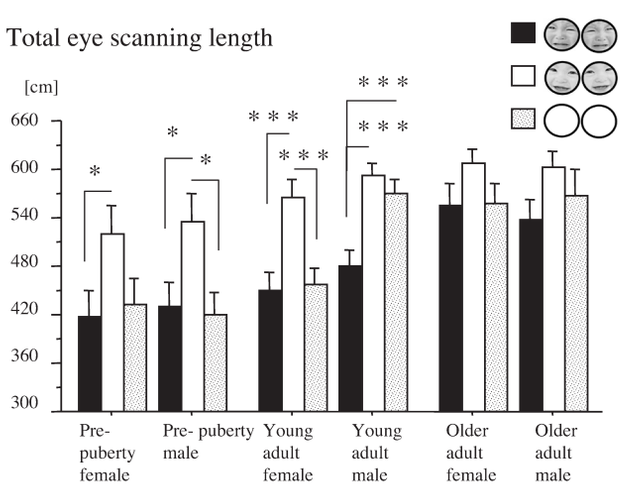

Fig. 3. Total eye scanning length (TESL; ordinate) at each session in three age groups (abscissa). Asterisks indicate significant differences between stimuli. *: p<0.05, ***: p<0.001

Young adult: The main gender difference by two-way ANOVA (gender × stimuli) was significant [F=11.9, p<0.0001], and the main stimulus difference was also significant [F=17.0, p<0.0001]. There was interaction observed between gender and stimuli (p<0.05). The TESL when viewing smiling babies was significantly longer than that of both the crying babies (p<0.0001) and the circles (p<0.01). By one-way ANOVA (gender), TESL of women when viewing the circles was significantly shorter [F=18.1, p<0.0001] than that of age-matched men. In women, TESL [F=10.4, p<0.0001] when viewing smiling babies was significantly longer than those for the crying babies (p<0.001) and the circles (p<0.001). In men, TESL [F=9.9, p<0.0001] when viewing smiling babies was significantly longer than those in crying babies (p<0.001) and TESL when viewing the circles was significantly longer than those in crying babies (p<0.01).

Older adult: The main gender difference by two-way ANOVA (gender × stimuli) was not significant, and the main stimulus difference was also not significant. There was no interaction observed between gender and stimuli (p=0.058). There were no gender differences observed by one-way ANOVA (gender). There was also no significant stimulus difference in elder women or men.

Total number of gazing points (Fig. 4)

Pre puberty: By two-way ANOVA, the main gender difference was not significant, but the main stimuli difference was significant [F=10.5, p<0.0001]. There was no interaction observed between stimuli and gender. The TNGP for simple circles of smiling babies was significantly larger than those of both the crying babies (p<0.001) and the circles (p<0.01).

Young adult: The main gender difference by two-way ANOVA was significant [F=17.7, p<0.0001] and the main stimuli difference was also significant [F=9.1, p<0.0001]. There was no interaction observed between stimuli and gender. By one-way ANOVA (stimuli), in women, TNGP of smiling babies was significantly larger than those of the crying babies (p<0.001). But, in men, there were not significant differences observed among three stimuli. By one-way ANOVA

(gender), TNGP of women when viewing the crying babies was significantly smaller than those of age-matched men [F=5.0, p<0.05]. By one-way ANOVA, TNGP of women when viewing the circles was significantly smaller than those of age-matched men [F=16.5, p<0.0001].

Older adult: The main stimuli difference by two-way ANOVA was significant, [F=3.8, p<0.05] and the main gender difference was not significant. There was no interaction observed between stimuli and gender. The TNGP of smiling babies was significantly larger than those of the circles (p<0.05).

Total number of transferring (between left and right fields)

Pre puberty: The main gender difference by two-way ANOVA (gender × stimuli) was not significant, but the main stimulus effect was significant [F=8.9, p<0.001]. There was no interaction. The number of transferring of the smiling babies was significantly larger than that of both the crying babies (p<0.0001) and the circles (p<0.01). By one-way ANOVA (stimuli), the number of transferring of girls when viewing smiling babies was significantly larger [F=5.3, p<0.01] than that of the crying babies (p<0.01) and the circles (p<0.05). By one-way ANOVA (stimuli), the number of transferring of boys when viewing smiling babies was significantly larger [F=4.0, p<0.05] than that of the crying babies (p<0.05) and the circles (p<0.05).

Young adult: The main gender difference by two-way ANOVA (gender × stimuli) was not significant, but the main stimulus effect was significant [F=23.4, p<0.0001]. The number of transferring of the smiling babies was significantly larger than that of both the crying babies (p<0.0001) and the circles (p<0.0001). By one-way ANOVA (stimuli), the number of transferring of women when viewing smiling babies was significantly larger [F=10.8, p<0.0001] than that of the crying babies (p<0.01) and the circles (p<0.0001). The number of transferring of women when viewing crying babies was significantly larger than that of the circles (p<0.05). The number of transferring of men when viewing smiling babies was significantly larger [F=16.3, p<0.0001] than that of the crying babies (p<0.0001) and the circles (p<0.0001). By one-way ANOVA (gender), the number of transferring of men when viewing circles was significantly larger [F=5.6, p<0.05] than that of age-matched women.

Older adult: The main gender difference and the main stimulus effects were not significant by two-way ANOVA (gender × stimuli). By one-way ANOVA (stimuli), the number of transferring of women when viewing smiling babies was significantly larger [F=4.8, p<0.05] than that of the crying babies (p<0.05) and the circles (p<0.001). By one-way ANOVA (stimuli), the number of transferring of older men when viewing smiling babies was significantly larger [F=4.0, p<0.05] than that of the crying babies (p<0.05) and the circles (p<0.01).

Left and right fields of screen (Fig. 5)

Pre puberty: The main gender difference by two-way ANOVA (gender × side) when viewing the simple circles was not significant, but the main field difference was significant [F=10.0, p<0.01]. There was no inter-

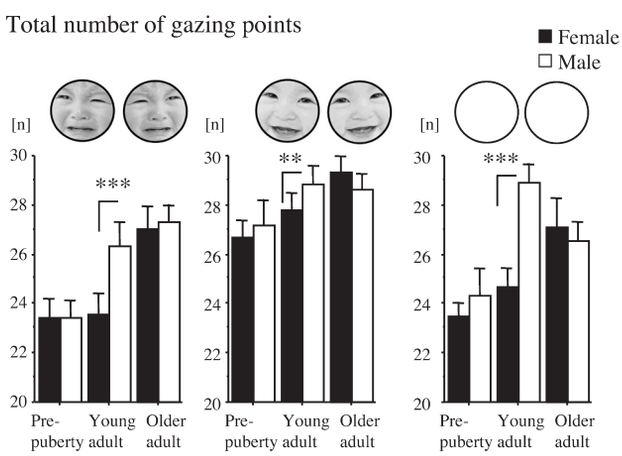

Fig. 4. Total number of gaze points (TNGP; ordinate) while viewing three stimuli, compared between genders and screen fields. Asterisks indicate significant differences between women and the men. *: p<0.05

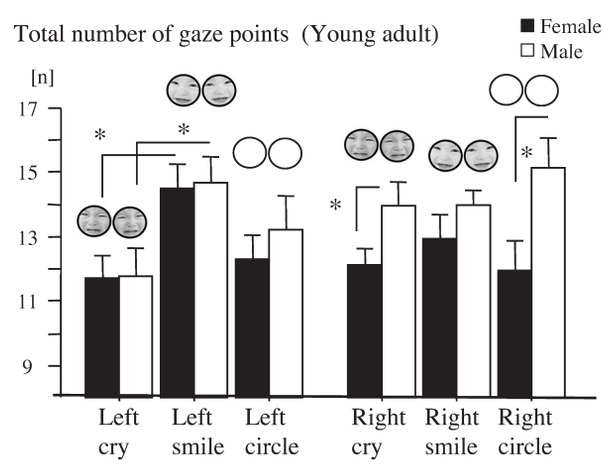

Fig. 5. Total number of gaze points (TNGP; ordinate) while viewing simple circles, compared between genders. Asterisks indicate significant differences between women and the men. *: p<0.05

action observed between gender and field. The TNGP in left field was significantly smaller [$p<0.01$] than those in right field.

Young adult: The main gender difference by two-way ANOVA (gender field) when viewing the crying babies was not significant, but the main field difference was significant [$F=6.0$, $p<0.05$]. There was no interaction observed between gender and group. The TNGP in left field was significantly smaller ($p<0.01$) than those in right field.

The main gender difference by two-way ANOVA (gender× field) when viewing the smiling babies was not significant, but the main field difference was significant [$F=9.0$, $p<0.01$]. There was no interaction observed between gender and group. The TNGP in right field was significantly smaller ($p<0.01$) than those in left field.

The main gender difference by two-way ANOVA (gender × side) when viewing the circles was significant [$F=11.3$, $p<0.0001$], but the main side difference was not significant. There was interaction observed between gender and side ($p<0.05$). The TNGP [$F=6.0$, $p<0.05$] of women in right side when viewing crying babies was significant shorter ($p<0.05$) than those in age-matched adult men as shown in Fig. 5. The TNGP [$F=14.6$, $p<0.001$] of women in right side when viewing circles was significant smaller ($p<0.001$) than those in age-matched men as shown in Fig. 5.

Older adult: The main gender difference by two-way ANOVA (gender × side) when viewing the crying babies was not significant but the main side difference was significant [$F=7.9$, $p<0.01$]. There was no interaction observed between gender and group. The TNGP in left side was significantly smaller ($p<0.01$) than those in right side.

DISCUSSION

The most important finding of the present study was that exploratory eye movements clearly differed between young adult women and men when viewing simple circles and crying babies only at right field, whether pre puberty or older adults did not; this suggests that exploratory eye movement is a useful biologic marker for evaluating the gender difference.

Kojima et al. [2,3] investigated exploratory eye movements using specially constructed S-shaped geometric figures, demonstrating that exploratory eye movement was a useful biologic marker of visual cognitive function in humans. In the present study, we found that exploratory eye movement of women showed properties similar to those previously Miyahira et al. [4] found that TESL in adult women was shorten than that in men. The present study also examined effects of affective stimuli on eye movements as well as gender difference in eye movements at different times of life. Specific aspects are discussed below.

Total eye scanning length (TESL)

TESL for women was significantly shorter than for men. The TESL when viewing the smiling babies was the longest among the three stimuli, followed by simple circles and then crying babies. Since significant gender differences in TESL were seen only when young adults viewed simple circles, scanning length may vary considerably with age. Young adults, and elderly persons, scanning length varied between age-defined groups for crying babies and simple circles, but not for smiling babies, suggesting that the former figures show more variability in response according to age than the latter. These findings also suggest that simple visual targets may be particularly useful for evaluating exploratory eye movement studies according to gender differences, as reported previously [4,18]. Findings might reflect method of visual response assessment, but one should consider that no significant changes among three life phases were seen when viewing the smiling babies.

Before puberty, TESL for crying babies, smiling babies, and circles did not show significant gender differences. In older adults, TESL also did not show significant gender differences. A gender difference for TESL was obtained only in younger adults, suggesting again that responses to these visual stimuli may be developmentally and/or hormonally dependent as reported previously [4,18].

The schismatic decussating of optic nerve fibers from the retina in humans ensures that each primary visual cortex receives input exclusively from the contralateral visual field. The source of gender difference could easily arise from a slightly slower scan [10], a longer decision time at each stage of scanning, or a more rapid decay of stored visual information in women [19].

In young adults, TESL of women on the right side when viewing the simple circles was significantly shorter than that of age-matched adult men, but TESL for the left field did not differ significantly between genders in young adults. In case of the mental rotation task, men showed a right-hemisphere advantage whereas women showed no hemisphere differences [20,21]. This laterality may indicate that the gender difference for TESL in adults viewing simple circles resulted from hemispheric functional differences.

Thus, the TESL on exploratory eye movements may be useful for an evaluation the hemispheric function of brain concerning gender differences.

Total number of gaze points (TNGP)

The right brain has been considered to role emotional functions, and the left-brain symbolic functions [14,22]. In the present study, difference of affective stimuli is obvious only at left fielding the screen, however, gender difference is only observed at right field. Schwartz et al. [20] reported that for emotion-linked images the eyes tended to move leftward, in contrast to rightward for other images; they concluded that this supported links between the right brain and emotional function. Furthermore, Gary et al. [22] reported that right-handed subjects tend to look to the left when answering affective questions, and concluded that the right hemisphere has special role in emotion in the intact brain. We showed that TNGP was smaller when young adult subjects of both genders viewed crying baby faces than when they viewed smiling baby faces, but only in the left field. Thus, the present observations which the effects of affection is significant only at left field on the screen, may be useful for an evaluation the hemispheric function of brain.

Women are considered to show a more cognitive balance between right and left-brain as reported previously [5,15,23].

Conclusions and physiologic significance

Significant gender differences were observed between young adult women and men when viewing the simple circles and the crying babes evaluation with exploratory eye moving. Shorter TESL and smaller TNGP in adult women were obtained to evaluate fixation points as subjects viewed the simple circles and the crying babies in preparation for copying them. No gender differences were seen in children and older adults, suggesting that exploratory eye movements may be influenced by gonadal hormones [24]. Both TESL and TNGP might be a gender marker, and TNGP might be a reflection of hemispheric function. Women appeared to gaze at certain parts of the circle with even balance between right and left fields, reflecting attentional focus.

Finally, exploratory eye movements while viewing certain pictures showed large differences between women and men in the right field, and marked differences among facial affection in the left field. Thus, exploratory eye movements appear to include gender and hemispheric functional markers helping to make them useful for exploring human visual cognition.

REFERENCES

1. Holzman PS, Solomon C, Levin S, and Waternaux CS. Pursuit eye movement dysfunction in schizophrenia: Family evidence for specificity. Arch Gen Psychiatry 1984; 41:136-139.
2. Kojima T, Matsushima E, Nakajima K, Shiraishi H, Ando K et al. Eye movement in acute, chronic, and remit schizophrenics. Biol Psychiatry 1990; 27:975-989.
3. Kojima T, Matsushima E, Ando K, and Ando H. Exploratory eye movement and neuro-psychological tests in schizophrenic patients. Schizophr Bul 1992; 18:85-94.
4. Miyahira A, Morita K, Yamaguchi H, Morita Y, Nonaka K et al. Gender differences of exploratory eye movements: a life span study. Life Science 2000; 68:569-577.
5. Ray WJ, Morell M, Frediani AW, and Tucker DM. Sex differences and lateral specialization of hemispheric functioning. Neuropsychologia 1976; 14:391-394.
6. Buchsbaum MS, Henkin RI, and Christiansen RL. Age and sex differences in averaged evoked responses in a normal population, with observation on patients with gonadal dysgenesis. Electro encephalogr Clin Neurophysiol 1974; 37:137-144.
7. David WL, and Charles SR. Sex differences in cognitive/motor overload in reaction time tasks. Neuropsychologia 1978; 16:611-616.
8. Delacoste UC, and Holloway RL. Sexual dimorphism in the human corpus callosum. Science 1982; 216:1413-1432.
9. Sheare DE, Emmerson RY, and Dustman RE. Gender differences in pattern reversal evoked potential amplitude; Influence of check size and single tarial response variability. Am J EEG Technol 1992; 32:196-203.
10. Efron R, Yund EW, and Nichols DR. Scanning the visual field without eye movements-A sex difference. Neurosychologia 1987; 125:617-644.
11. Cohn NB, Kircher J, Emmerson RY, and Dustman RE. Pattern reversal evoked potentials: Age, sex and hemispheric asymmetry. Electroencephalogr Clin Neurophysiol 1985; 62:399-405.
12. McGlone J. Sex differences in functional brain asymmetry. Cortex 1978; 14:122-128.
13. Yamamoto M, Morita K, Waseda Y, Ueno T, and Maeda H. Changes in auditory p300 with clinical remission in schizophrenia; Effects of facial-affect stimuli. Psychiatry Clin Neuroscience 2001; 55:347-352.
14. Diamond M, Diamond AL, and Mast M. Visual sensitivity and sexual arousal levels during the menstrual cycles. J Nerv Ment Dis 1972; 155:170-176.
15. Tucker DM. Sex differences in hemispheric specialization for synthetic visuospatial function. Neuropsychologia 1976; 14:447-454.
16. Lang SF, Nelson CA, and Collins PF. Event-related potentials to emotional and neutral stimuli. J Clin Exp Neuropsychol 1990; 12:946-958.
17. Kojima T. A study of eye movements in patients with endogenous depression in comparison with chronic schizophrenics, neurotics and normal subjects. Seishin 1972; 74:511-535. (in Japanese)
18. Miyahira A, Morita K, Yamaguchi H, Morita Y, and Hisao M. Gender differences and reproducibility in exploratory

eye movements of normal subjects. Psychiatry Clin Neurosci 2000; 54:31-36.
19. Bakan P, and Utnam W. Right-left discrimination and brain materialization: sex differences. Arch Neurol 1974; 30: 334-335.
20. Schwartz GE, Davidson RJ, and Maer F. Right hemisphere lateralization for emotion in the human brain: uneractions with cognition. Science 1975; 190:286-288.
21. Siegel-Hinson RL, and McKeever WF. Hemisphreic specialization, spatial activity experience, and sex differences on tests of mental rotation ability. Laterality 2002; 7:59-74.
22. Gary ES, Richard JD, Foster M, Right hemisphere lateralization for emotion in the human brain: Interaction with cognition. Science 1975; 190:286-288.
23. Rilea SL, Roskos-Ewoldsen B, and Boles D. Sex differences in spatial ability: A lateralization of function approach. Brain Cogn 2004; 56:332-343.
24. Dimond SJ, Farrington L, and Johnson P. Differing emotional response from right and left hemispheric. Nature 1976; 261:690-692.

Case Report

Kurume Medical Journal, 54, 95-99, 2007

Serial Magnetic Resonance Imaging and Single Photon Emission Computed Tomography Study of Acute Disseminated Encephalomyelitis Patient after Japanese Encephalitis Vaccination

TAKASHI OHYA, SHINICHIRO NAGAMITSU, YUSHIRO YAMASHITA AND TOYOJIRO MATSUISHI

Department of Pediatrics and Child Health, Kurume University School of Medicine, Kurume 830-0011, Japan

Received 9 October 2007, accepted 16 January 2008

Summary: We report a 5-year-old mentally retarded Japanese boy who developed acute disseminated encephalomyelitis (ADEM) two weeks after Japanese encephalitis vaccination (Beijing strain). He presented sudden status epilepticus, fever, and disturbance of consciousness. Initial neuroradiological findings revealed multifocal cortical swellings without any white matter lesions, suggesting the existence of partial encephalitis or focal status epilepticus. On the follow-up neuroradiological examinations, small white matter lesions were identified as having gradually extended in spite of clinical improvement by methylprednisolone pulse therapy. The cortical involvement became temporarily worse along with the extension and delayed appearance of white matter lesions. Single photon emission computed tomography (SPECT) showed marked hypoperfusion of cerebral blood flow (CBF) in the cortical lesions at both the acute and the recovery period. The serial neuroradiological findings indicated involvement of white matter and gray matter regions at different stages of the illness and a delay between the onset of symptoms and the appearance of ADEM-associated MR imaging of white-matter lesions.

Key words ADEM, JE vaccination, ADEM-associated MR imaging

INTRODUCTION

Japanese encephalitis (JE) is one of the most common causes of epidemic viral encephalitis in the world, especially in South-East Asia. The annual incidence and mortality estimates for JE in South-East Asia are 30,000-50,000 and 10,000, respectively. However, this figure might be an underestimate, one study estimated the annual incidence at 175,000 per year [1]. The number of patients with JE in Japan was several thousand per year in the 1950's. Beginning in 1967, vaccination was actively recommended, the incidence was about a dozen per year in the 1980's and several per year after 1992 [2].

Acute disseminated encephalomyelitis (ADEM) is an acute demyelinating disorder of the central nervous system. It usually follows an infection or vaccination. It is clinically characterized by the acute or subacute onset of a multifocal neurological disturbance that typically follows a monophasic course. MRI findings typically reveal multifocal increased signal intensities on T2-weighted image in the white matter, subcortical white matter, basal ganglia, brainstem, or spinal cord [3]. Fourteen cases of ADEM after JE vaccination have been reported since 1991 in Japan [4]. Because some cases were severe, the Japanese Ministry of Health, Labor and Welfare recommended a suspension of JE vaccination in May, 2005.

Here we report a patient having ADEM associated with JE vaccination who showed atypical neuroradiological findings in the various stages of the illness.

Corresponding author: Toyojiro Matsuishi M.D., Ph.D, Department of Pediatrics and Child Health, Kurume University School of Medicine, 67 Asahi-machi, Kurume 830-0011, Japan. Tel: 81-942-31-7565 Fax: 81-942-38-1792 E-mail: tmatsu@med.kurume-u.ac.jp

Abbreviations: ADEM, acute disseminated encephalomyelitis; CBF, cerebral blood flow; CSF, cerebrospinal fluid; JE, Japanese encephalitis; SPECT, single photon emission computed tomography.

CASE REPORT

A 5-year-old mentally retarded boy suddenly developed generalized tonic-clonic seizure that lasted about 60 min, 2 weeks after his third JE vaccination was administered. He had been diagnosed as having delayed motor milestones, mental retardation (developmental quotient: 27), congenital anomalies of the trachea (tracheobronchial malacia, stenosis of the left main trachea), and asthma. Screening for inborn errors of metabolism was negative. Chromosome study revealed normal male karyotype. He was allergic to soybeans, wheat and corn before the onset of this episode. There was no family history of epileptic, neuromuscular, metabolic, collagen-related, vascular or demyelinating disorders. He had previously received vaccinations for measles, BCG, rubella, polio, chickenpox and mumps without any complications.

When he was admitted to Kurume University Hospital with status epilepticus, he had fever, dyspnea with wheeze, and disturbance of consciousness. No meningeal signs were observed. The peripheral white blood cell count was increased (32400 /mm^3) and C-reactive protein was positive (6.76 mg/dl). Serum levels of electrolites, glucose, transaminase and ammonium were normal. Cerebrospinal fluid (CSF) contained leukocytes at 3 /mm^3, all leukocytes were mononuclear cells. Total protein and myelin basic protein (MBP) in the CSF were 20 mg/dl and 377 pg/ml (normal<102 pg/ml), respectively. No IgG oligoclonal band was detected. We examined JE virus hemagglutination inhibited titers and IgM (enzyme-immunoassay) of varicella-zoster virus, herpes simplex virus, cytomegalovirus and Mycoplasma pneumoniae (Particle agglutination) in CSF. They were all negative. Brain CT on admission revealed no hemorrhage or cortical edema. Electroencephalogram at 3 days of illness revealed diffuse high-amplitude delta waves without any focal epileptic discharge. At 6 days of illness, neuroradiological examinations including brain

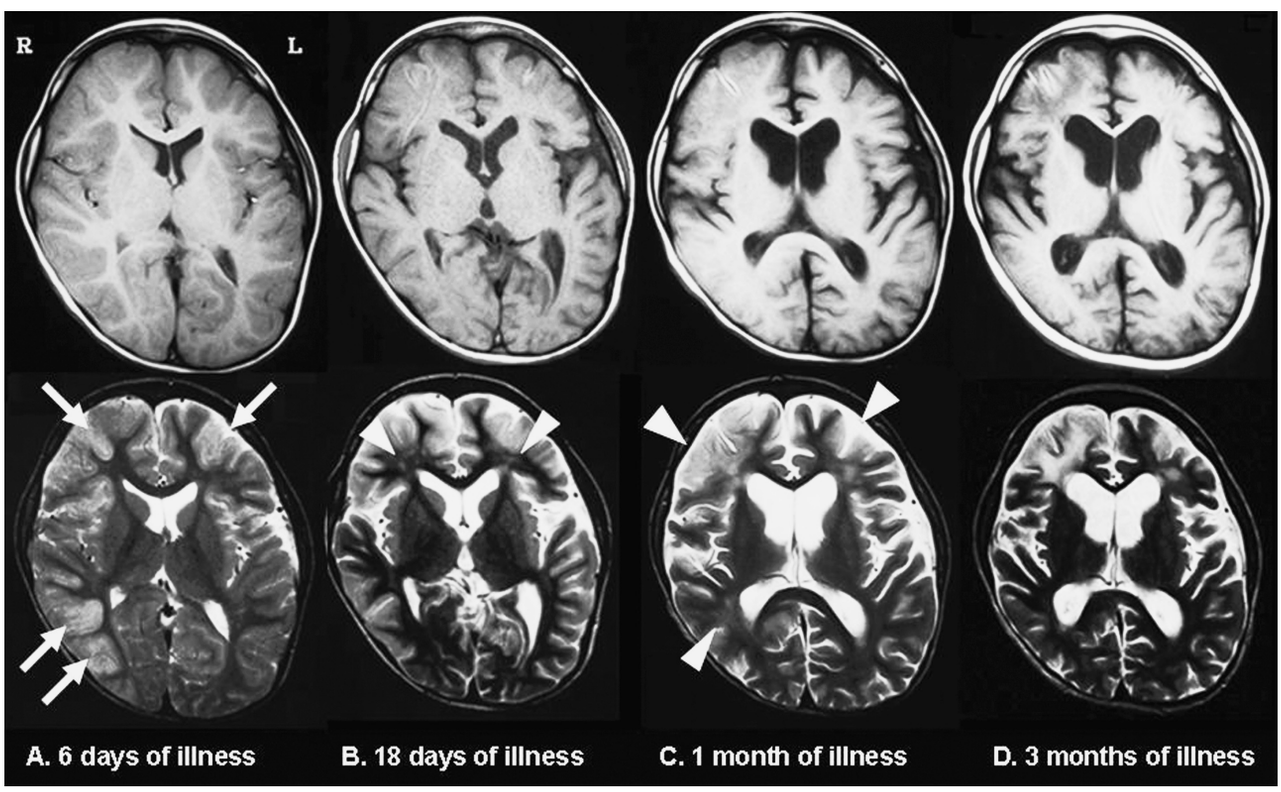

Fig. 1. Magnetic resonance imaging of the brain. Upper row: T1-weighted MR imaging. Lower row: T2-weighted MR imaging. A. 6 days of illness. Cortical swellings with increased signal intensities in T2-weighted axial imaging appear in the bilateral frontal and right occipital regions (arrows). B. 18 days of illness. The cortical swelling is diminished in the bilateral frontal and right occipital regions. Increased signal intensities in the bilateral frontal white matter appear in the T2-weighted imaging (arrowheads). C. 1 month of illness. The cortical swelling and white matter lesions of bilateral frontal lobes and right occipital lobe have worsened again. (arrowheads). Marked cerebral atrophy is also seen. D. 3 months of illness. The cortical lesions have disappeared and the white matter lesions remained behind. R: right, L: left.

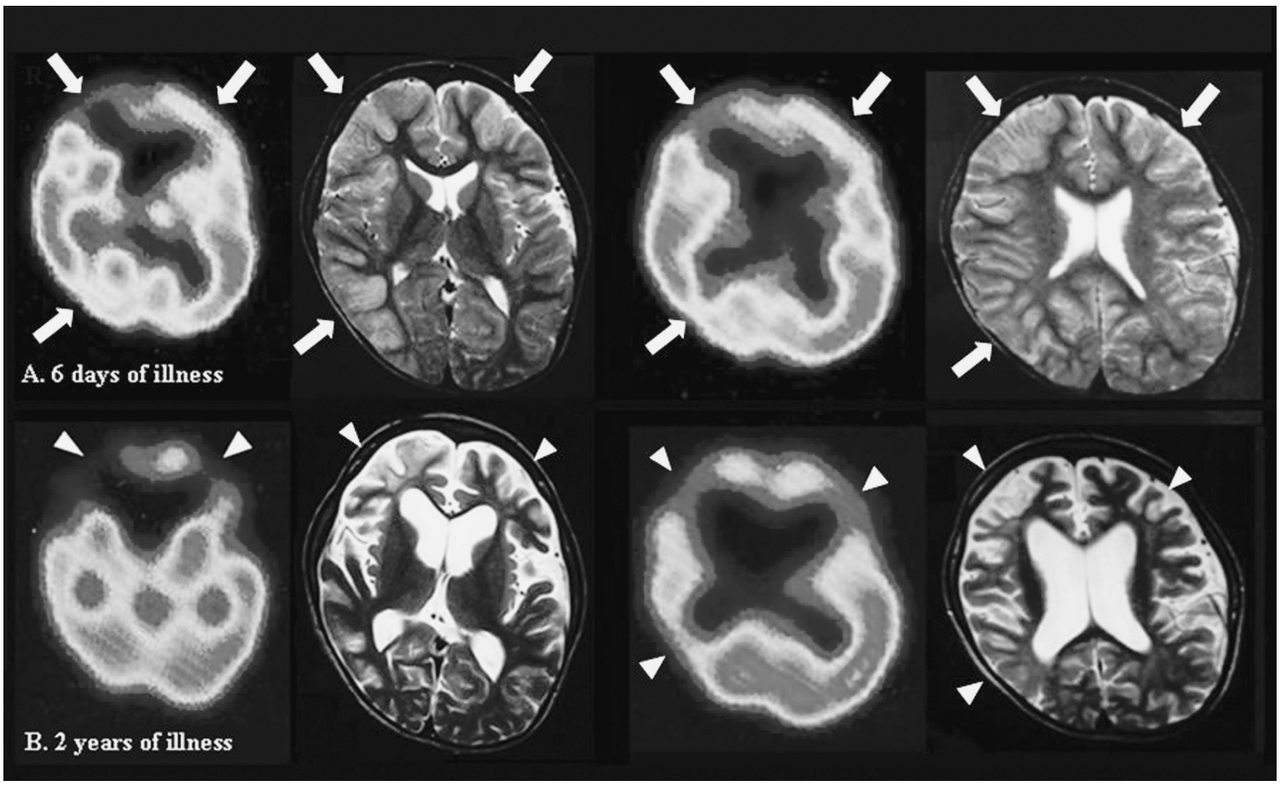

Fig. 2. ^{123}I-IMP single photon emission computed tomography and T2-weighted MR imaging. Upper row: At 6 days of illness; ^{123}I-IMP SPECT showed decreased cerebral blood flow (CBF) in the bilateral frontal, right occipital, and right parietal regions, where these regions had cortical swellings on MRI (arrows). In frontal regions, CBF was much decreased in the right. Lower row: At 2 years of illness; MRI showed the cortical and white matter lesions in the bilateral frontal and right parietal regions where ^{123}I-IMP SPECT showed decreased CBF (arrowheads).

CT, MRI, ^{123}I-IMP single photon emission computed tomography (SPECT) were performed. Brain CT revealed poor differentiation between the cortex and the white matter, and MRI showed focal cortical swellings in the bilateral frontal and right occipital regions (Fig. 1A). ^{123}I-IMP SPECT showed decreased cerebral blood flow (CBF) in the bilateral frontal, right occipital, and right parietal regions , where these regions had cortical swellings on MRI (Fig. 2A). In frontal regions, CBF was much decreased in the right. Although we examined MRI of the spinal cord, it was normal at acute phase.

Initially, we suspected partial encephalitis or focal status epilepticus based on clinical symptoms and neuroradiological findings, thus, we treated the patient with intravenous administration of an antiepileptic agent and mannitol to lower intracranial pressure. However, we could not deny the existence of ADEM on account of the recent vaccination, therefore, we started methylprednisolone pulse therapy (dose; 30 mg/kg/day, 3 days a week, total 9 times) at 7 days of illness. On the follow-up MRI at 18 days of illness, increased signal intensities in the bilateral frontal white matter were identified on the T2-weighted image (Fig. 1B), the size of these lesions showed gradual increase at 1 and 3 months of illness (Fig. 1C, D). In addition, the signal intensity in the right occipital region was increased at 1 month of illness (Fig. 1C). The focal cortical swellings in the bilateral frontal and right occipital regions were decreased at 18 days of illness, however, these regions seemed to swell again along with enlargement or delayed appearance of white matter lesions at 1 month of illness before disappearing at 3 months of illness (Fig. 1A-D). At 3 months of illness, the white matter lesions remained behind (Fig. 1D). The patient's consciousness was gradually improved at 3 days after the beginning of the methylprednisolone pulse therapy. He could smile at 9 days, maintain a sitting position at 14 days, and stand up at 24 days after the therapy. After methylprednisolone pulse therapy, prednisolone (1 mg/kg/day) was orally administered, the medication was tapered and discontinued within six months. He has shown no neurological sequel except intractable complex partial seizures with multifocal spikes.

On the follow-up neuroradiological examination

at 2 years of illness, MRI showed marked cortical atrophy predominantly in the bilateral frontal and temporal regions (Fig. 2B). MRI also showed the cortical and white matter lesions in the bilateral frontal and right parietal regions where ^{123}I-IMP SPECT showed decreased CBF (Fig. 2B).

DISCUSSION

The incidence of severe neurological complications associated with JE vaccination has been reported to be 1-2.3 per million vaccinations [5]. We previously reported seven cases of ADEM after JE vaccination [4], in which various neurological symptoms such as seizure, disturbance of consciousness, paralysis, gait disturbance, and headache, were seen. Initially, we suspected our patient of having partial encephalitis or focal status epilepticus based on his clinical symptoms and initial neuroradiological findings. However, the serial neuroradiological findings–in particular, the late appearance of abnormal signal intensities in the white matter regions, the history of JE vaccination, good clinical response to methylprednisolone therapy, and good clinical prognosis–confirmed the existence of ADEM in this patient. We also could determine that the patient did not have cerebral infarction or a progressive white matter disease such as metachromatic leukodystrophy, adrenoleukodystrophy, Krabbe disease and other metabolic demyelinating diseases.

According to the previous literature, MRI findings of ADEM after JE vaccination typically reveal multifocal lesions predominantly in the deep white matter, thalamus, cerebellum and optic nerve, generally identified at the early stage of neurological symptoms [4]. In our case, we could detect a few characteristic MRI findings in the serial examinations. First, multifocal cortical swellings without the white matter legions were found at the onset of neurological symptoms. Second was the late appearance of white matter lesions in spite of the improvement of clinical symptoms. Third, the cortical swellings became worse temporarily along with the enlargement or appearance of white matter lesions.

It is known that MRI findings of patients with generalized tonic-clonic seizure or status epilepticus reveal transient changes including focally increased T2 signal intensity, swelling, and increased volume of the involved cortical gyrus due to seizure-induced transient cytotoxic and vasogenic cerebral edema [6,7]. In our case, the initial cortical swellings and their diminutions between 6 days and 18 days of illness may reflect transient cortical edema due to prolonged seizure activity. On the other hand, white matter lesions on MRI obtained from some patients with ADEM have been reported to appear shortly after symptom onset [8,9]. Honkaniemi et al. [8] reported three cases of ADEM in which white matter lesions did not appear until several weeks after the onset of the disease and increased during the recovery period. Kimura et al. [9] also reported that initial MR imaging failed to show ADEM-related lesions in children with postinfectious encephalitis. Although ADEM is typically described as affecting the white matter, gray matter involvement is not unusual because it also contains myelin [3,10]. Taken together, the delayed appearance of white matter lesions during a phase in which clinical symptoms was absent may indicate ADEM-related demyelination. The pathological mechanism of the delay between the neuroradiological findings and neurological symptoms remains unknown. It is important to know that both white matter and gray matter are involved at different stages of the illness and that consecutive neuroradiological evaluation is necessary if the clinical picture is suggestive for ADEM.

Because of the delay between the onset of symptoms and the appearance of ADEM-associated MR imaging, SPECT has contributed to identification of regions with functional deficits at different stages of the disease [11-13]. Okamoto et al. [12] reported that persistent hypoperfusion both at rest and in response to acetazolamide administration remained even after disappearance of hyperintensive lesions from MRI, suggesting persistent impairment of cerebral circulation affecting cognitive abilities. A previous HMPAO-SPECT study of a patient with ADEM revealed a combined pattern of hyper and hypoperfusion regions and the presence of inflammatory cells and cortical deactivation secondary to disconnection from the subcortical structures, respectively [13]. Serial SPECT study in our case showed persistent hypoperfusion in several cortical regions indicating impairment of cortical activity, which resulted from the decreased volume of the involved cortical gyrus. We cannot always detect these abnormalities on MRI. We considered that it is useful to follow serial SPECT.

In conclusion, serial MRI and SPECT may contribute to assessing the involvement of lesions and functional impairment at different stages of the disease.

REFERENCES

1. Tsai TF. New initiatives for the control of Japanese encephalitis by vaccination: minutes of a WHO/CVI meeting, Bangkok, Thailand, 13-15 October 1998. Vaccine 2000; 18

Suppl 2:1-25.
2. Arai S, Taya K, Okabe N, Takasaki T, and Kurane I. Japanese encephalitis in Japan. Rinshou to Uirusu 2004; 32:13-22. (in Japanese)
3. Hynson JL, Kornberg AJ, Coleman LT, Shield L, Harvey AS et al. Clinical and neuroradiologic features of acute disseminated encephalomyelitis in children. Neurology 2001; 56:1308-1312.
4. Ohtaki E, Matsuishi T, Hirano Y, and Maekawa K. Acute disseminated encephalomyelitis after treatment with Japanese B encephalitis vaccine (Nakayama-Yoken and Beijing strains). J Neurol Neurosurg Psychiatry 1995; 59:316-317.
5. Inactivated Japanese encephalitis virus vaccine. Recommendations of the Advisory Committee on Immunization Practices (ACIP). MMWR Recomm Rep 1993; 42:1-15.
6. Kim JA, Chung JI, Yoon PH, Kim DI, Chung TS et al. Transient MR signal changes in patients with generalized tonicoclonic seizure or status epilepticus: periictal diffusion-weighted imaging. AJNR Am J Neuroradiol 2001; 22:1149-1160.
7. Kramer RE, Luders H, Lesser RP, Weinstein MR, Dinner DS et al. Transient focal abnormalities of neuroimaging studies during focal status epilepticus. Epilepsia 1987; 28:528-532.
8. Honkaniemi J, Dastidar P, Kahara V, and Haapasalo H. Delayed MR imaging changes in acute disseminated encephalomyelitis. AJNR Am J Neuroradiol 2001; 22:1117-1124.
9. Kimura S, Nezu A, Ohtsuki N, Kobayashi T, Osaka H et al. Serial magnetic resonance imaging 1996; 18:461-465.
10. Murthy SN, Faden HS, Cohen ME, and Bakshi R. Acute disseminated encephalomyelitis in children. Pediatrics 2002; 110:e21.
11. Hung KL, Liao HT, and Tsai ML. Postinfectious encephalomyelitis: etiologic and diagnostic trends. J Child Neurol 2000; 15:666-670.
12. Okamoto M, Ashida KI, and Imaizumi M. Hypoperfusion following encephalitis: SPECT with acetazolamide. Eur J Neurol 2001; 8:471-474.
13. Broich K, Horwich D, and Alavi A. HMPAO-SPECT and MRI in acute disseminated encephalomyelitis. J Nucl Med 1991; 32:1897-1900.

Original Contribution

Kurume Medical Journal, 54, 73-76, 2007

Dose-Dependent Effects of Recombinant Human Interleukin-11 on the Systemic Hemodynamic Function and Urination

KANEATSU HONMA*, **, NANCY L. KOLES**, HASAN B. ALAM†
JAMES C. KEITH Jr.‡ AND MATTHEW POLLACK**

Division of Operative Management, Koga Hospital 21, Kurume 839-0801, Japan, Departments of Medicine and Surgery†, Uniformed Services University of the Health Sciences, F. Edward Hebert School of Medicine, Bethesda MD 20814 and ‡Wyeth Research, Andover MA 01810, USA*

Received 16 November 2007, accepted 9 January 2008

Edited by HISAO IKEDA

Summary: The purpose of this study was to determine whether recombinant human interleukin-11 (rhIL-11) could dose-dependently improve the hemodynamic function. Using a swine hemorrhagic shock model, rhIL-11 was given at the beginning of resuscitation. The animals were randomized to receive a single dose of rhIL-11 (5, 20, or 50 μg/kg, group I to Ⅲ for respectively) or saline (group Ⅳ). Blood, urine and both pleural and peritoneal effusion were thus obtained and analyzed. The mean arterial pressure (MAP) was higher post-resuscitation (PR) in group Ⅲ (62.9±8.2 mmHg) than in groups I, Ⅱ and Ⅳ (54.9±1.7, 53.9±4.3, 55.9±9.4 mmHg, respectively) ($P<0.01$). The urine output (I: 999±428, Ⅱ: 1249±180, Ⅲ: 1434±325, Ⅳ: 958±390 ml) and the cardiac output (CO) (I: 3.01±0.66, Ⅱ: 3.30±0.49, Ⅲ: 3.43±0.57, Ⅳ: 2.73±0.49 L/min.) increased in a dose dependent manner of rhIL-11. CO level and urine output were significantly higher in group Ⅲ than in group Ⅳ ($P<0.05$). In addition, the volume of third space fluid loss (pleural and peritoneal effusion) of group Ⅲ was significantly lower than other groups (I: 157±32, Ⅱ: 138±32, Ⅲ: 82±21, Ⅳ: 125±32 ml) ($P<0.05$). In conclusion, even a low dose of rhIL-11 improved the hemodynamic functions dose-dependently in a porcine model of hemorrhagic shock, although the relationship did not demonstrate a simple linearity.

Key words recombinant human interleukin-11, hemorrhagic shock, effusion, urination, dose-dependent

INTRODUCTION

Interleukin-11 (IL-11), a multi potential cytokine, exhibits anti-inflammatory and protective activities in a variety of in vivo and in vitro models [1,2]. Our previous study demonstrated that the administration of recombinant human interleukin-11 (rhIL-11) (50 μg/kg) improved the levels of mean arterial pressure (MAP) and urine output, and reduced the amount of third space fluid loss in a hemorrhagic shock model of rats and swine. We hypothesized that the increasing vascular permeability in hemorrhagic shock might therefore be inhibited by rhIL-11 [3]. However, we did not determine whether these beneficial effects of rhIL-11 were dose dependent. The purpose of this study was to determine whether rhIL-11 could improve both the MAP and urine output, and also decrease the amount of third space fluid loss in a dose-dependent manner in a swine hemorrhagic shock model.

MATERIALS AND METHODS

The institutional Laboratory Animal Review Board for the care and use of animals approved this study. All

Corresponding author: K. Honma, Division of Operative management, Koga Hospital 21, 3-3-8 Miyanojin, Kurume 839-0801, Japan. Tel: 0942-38-3333 Fax: 0942-38-2946 E-mail: khonma@tc5.so-net.ne.jp

Abbreviations: CO, cardiac output; IL-6, interleukin-6; IL-11, interleukin-11; rhIL-11, recombinant human interleukin-11; MAP, mean arterial pressure; PMN, neutrophil; PR, post-resuscitation; R, resuscitation.

research was conducted in compliance with the Animal Welfare act and other Federal statutes and regulations relating to the animals and experiments involving animals. This study adhered to the principles stated in the Guide for the Care and Use of Laboratory Animals, NIH publication no. 86-23, 1985 edition.

Animal surgery

Yorkshire swine (25-35 kg) were fed a standard diet, and food was withheld the night before the experiment. Anesthesia was induced with an intramuscular injection of ketamine (10 mg/kg) and then the swine inhaled isoflurane and intubated. The animals were allowed to breath spontaneously using a Narkomed 2A ventilator (North American Dräger, Telford, PA). Under aseptic conditions, the right carotid artery and a branch of the external jugular vein were cannulated with a 16-gauge angiocatheter and 8.5F introducer catheter sheaths, respectively. A 7.5-Fr oximetric thermodilution pulmonary artery catheter (Edwards Lifesciences LLC, Irvine, CA) was positioned in the pulmonary artery through the introducer sheath. Urine was collected using a catheter that was surgically placed in the bladder. Based on a volume-controlled porcine model of hemorrhagic shock, bleeding was induced at a rate of 28 ml/kg (approximately 40% of the estimated total blood volume) in all animals during a 15-min period through the carotid artery line. The animals were thereafter maintained in a state of hypovolemic shock for 60 min, and then were injected with the designed dose of rhIL-11 (Wyeth Research, Andover, Massachusetts) at the beginning of resuscitation with 0.9% sodium chloride solution (3 × shed blood volume), over a period of one hr and then were observed for an additional 6 hrs. The animals were randomly assigned into 5 μg/kg (Group I, n= 6), 20 μg/kg (Group Ⅱ, n=5), 50 μg/kg (Group Ⅲ, n=6), saline control (Group Ⅳ, n=7)

Blood and urine samples were obtained and analyzed at baseline, at the end of hemorrhaging, and thereafter once every an hour. Urine specific gravity was analyzed at the time period of baseline, resuscitation one hour and post resuscitation 6 hrs. The amounts of both pleural and peritoneal effusion were precisely quantified using the clinically accepted criteria at the time of sacrifice.

Statistical analyses

All data are represented as the group means ± S.D. The Instat statistical software package (GraphPad Software, Inc., San Diego, CA) was used for inter-group comparisons. The parametric data were analyzed by an analysis of variance (ANOVA). Significance was defined as $P<0.05$.

RESULTS

Mean Arterial Pressure (MAP)

The MAP of Group Ⅲ was significantly higher than other groups following resuscitation (I: 54.9±1.7, Ⅱ: 53.9±4.3, Ⅲ: 62.9±8.62, Ⅳ: 55.9±9.4 mmHg, $P<0.01$), as shown in Table 1.

Urine output

The total urine output is shown in Table 2. The urine output improved dose-dependently (I: 999±428, Ⅱ: 1249±180, Ⅲ: 1434±325, Ⅳ: 958±390 ml). The urine output was a significantly higher in group Ⅲ than in group Ⅳ ($P<0.05$).

Effusion volume

The effusion volume (pleural and peritoneal effu-

TABLE 1.
Effect of rhIL-11 on MAP in hemorrhagic shock in pigs

Groups	n	Mean±SEM
I (rhIL-11: 5 μg/kg)	6	54.9±1.7 mmHg
Ⅱ (rhIL-11: 20 μg/kg)	5	53.9±4.3 mmHg
Ⅲ (rhIL-11: 50 μg/kg)	6	62.9±8.2 mmHg*
Ⅳ (saline control)	7	55.9±9.4 mmHg

*$P<0.01$
P values refer to the level of statistical significance regarding the observed differences in the MAP at 6 h post-resuscitation among the animals in study groups I, Ⅱ, Ⅳ and Ⅲ.

TABLE 2.
Urine output of the resuscitation period, and the volume of effusion (pleural and peritoneal) at the time of sacrifice (mean ± SEM)

Groups	n	Urine output (Resuscitation time 0 ~ Post-resuscitation time 6 h [mL])	Third space fluid loss (mL)
I	6	999±428	156.5±84.8
Ⅱ	5	1249±180	137.6±52.3
Ⅲ	6	1434±325*	82.0±21.0*
Ⅳ	7	958±390*	125.2±32.0

*$P<0.05$
P values refer to the level of statistical significance of observed differences in urine output (Ⅲ and Ⅳ), and in third space fluid loss among animals in study groups I, Ⅱ, Ⅳ and Ⅲ.

TABLE 3.
Urine specific gravity (mean±SEM)

Groups	n	Baseline	Resuscitation time 1 h	Post resuscitation time 6 h
I	6	1.012±0.004	1.007±0.001	1.018±0.008
II	5	1.008±0.003	1.004±0.001	1.017±0.002
III	6	1.007±0.004	1.004±0.001*	1.017±0.007
IV	7	1.011±0.006	1.005±0.001	1.015±0.003

P<0.05
P values refer to the level of statistical significance of observed differences in urine specific gravity at the time period of end-resuscitation among animals in study groups I, IV and III.

TABLE 4.
Cardiac output (L/min [mean±SEM])

Groups	n	Baseline	Shock (0 min)	Shock (60 min)	Resuscitation (60 min)	Post-resuscitation (60-180 min)	Post-resuscitation (240-360 min)
I	6	4.38±0.46	1.07±0.35	2.12±0.35	4.87±0.99	3.16±0.55	3.01±0.66*
II	5	4.45±0.73	1.47±0.49	2.43±0.36	5.53±0.72	3.40±0.43	3.30±0.49*
III	6	4.57±0.73	1.11±0.21	2.32±1.11	5.33±1.00*	3.36±0.45	3.43±0.57*
IV	7	3.98±0.66	1.10±0.38	1.85±0.46	4.79±0.95*	3.11±0.49	2.73±0.49*

*P<0.05
P values refer to the level of statistical significance regarding the observed differences in CO at the time period of post-resuscitation in study groups II, III and IV, I and III, and of resuscitation in groups III and IV. CO tended to increase dose-dependently at the time period of resuscitation and post-resuscitation.

sion) was shown in Table 2. There were no significant differences in the volume of peritoneal and pleural effusion between among groups I, II and IV (I: 157±85, II: 138±57, IV: 125±32 ml). But the effusion volumes were significant lower in other groups (P<0.05).

Urine specific gravity

Urine specific gravity at the time period of resuscitation 1 hr in group III (1.004) was significant lower than in groups I and IV (P<0.05), as shown in Table 3.

Cardiac output (CO)

The CO (I: 3.01±0.66, II: 3.30±0.49, III: 3.43±0.57, IV: 2.73±0.49 L/min.) increased dose-dependently. CO was significant higher in group II and III than in group IV, and significant higher in group III than group I, as shown in Table 4.

DISCUSSION

IL-11 is a multifunctional cytokine that shows a variety of effects, including anti-inflammatory, immunomodulatory, and cytoprotective effects in several animal models [1,2]. We previously demonstrated that 50 μg/kg of rhIL-11 injected at the beginning of resuscitation improved the systemic hemodynamic function in a swine hemorrhagic shock and resuscitation model [3]. Based on our previous data, we suggested that rhIL-11 might be a factor that plays an important role in regulating the vessel permeability and the systemic hemodynamic function. Regarding the contractile properties of the gut, the dose-dependent effects of rhIL-11 in rabbits colitis model have been reported [4]. However, so far no controlled studies demonstrating a dose-dependent effect of rhIL-11 on the systemic hemodynamic function have yet been reported.

Our data revealed that the urine output of these four groups increased dose-dependently of rhIL-11, while the third space fluid loss tended to decrease dose dependently. MAP was higher post-resuscitation (PR) in group III than in group I, II and IV. CO was improved dose dependently by rhIL-11 in the PR period and was significant higher in groups II, III than in group IV, and higher in group III than in group I. Although our data did not show any significant differences between the groups receiving low dose injection regarding MAP, urine output, or third space fluid loss, these data nev-

ertheless did show a dose-dependent tendency. This might be due to the small number of subjects studied or the low dose of rhIL-11in our study.

Depoortere et al. [4] demonstrated that rhIL-11 treatment dose-dependently decreased the inflammation in the colon, but the highest dose (720 μg/kg) of rhIL-11 only enhanced the body weight loss in comparison to the nontreated inflamed colitis rabbits. They also showed that the inflammation effect was normalized with the lowest dose of rhIL-11 in the proximal part of the colon, whereas in the distal part of the colon, the highest dose was needed. These data suggested that both a dose dependent effective site and a dose independent effective site thus exist in the gut. In our rat model, 100 μg/kg of rhIL-11 improved the systemic hemodynamic function and produced a marked reduction in the interleukin-6 (IL-6) mRNA expression (unpublished data). A large dose of rhIL-11 is suggested to more strongly restore the increased vascular permeability, while also normalizing tissue edema and body weight during hemorrhagic shock and resuscitation. It is currently accepted that neutrophils (PMN), which are activated by IL-6, are believed to be present in the microvasculature of end organs, thus releasing cytotoxic proteases and oxygen radicals that injure the endothelium and cause vascular leakage, tissue edema, and eventually organ injury and failure [5,6]. In addition, the local proinflammatory effects of IL-6 on PMN infiltration and organ damage in hemorrhagic shock have also been demonstrated [7]. This present study did not evaluate the changes in IL-6 mRNA during hemorrhagic shock. Further studies with a larger number of subjects and a larger dose of rhIL-11 are thus needed. In addition, further investigation regarding whether rhIL-11 dose-dependently reduce the IL-6 mRNA expression or the lipopolysaccharide-induced production of proinflammatory cytokines, or nitric oxide from macrophages [1] are also desirable.

In conclusion, even in a low dose administration of rhIL-11, rhIL-11 improved the systemic hemodynamic function and urine output dose-dependently, thereby reducing the degree of third space fluid loss following hemorrhagic shock and resuscitation, although the relationship did not demonstrate a simple linearity.

ACKNOWLEDGMENTS: This study was supported by an Office of Naval research Grant #N00014-03-MP-2-0057.

REFERENCES

1. Trepicchio WL, Ozawa M, Walters IB, Kikuchi T, Gilleaudeau P et al. Interleukin-11 therapy selectively downregulates type I cytokine proinflammatory pathways in psoriasis lesions. J Clin Invest 1999; 104:1527-1537.
2. Booth D, and Potten CS. Protection against mucosal injury by growth factors and cytokines. J Nat'l Cancer Inst Monogr 2001; 29:16-20.
3. K Honma, Koles NL, Alam HB, Rhee P, Rollwagen FM et al. Administration of recombinant Interleukin-11 improves the hemodynamic functions and decreases third space fluid loss in a porcine model of hemorrhagic shock and resuscitation. Shock 2005; 23:539-542.
4. Depoortere I, Thijs T, Assche GV, Keith Jr. JC, and Peeters TL. Dose-dependent effects of recombinant human interleukin-11 on contractile properties in rabbit 2,4,6-trinitrobenzene sulfonic acid colitis. J Pharmacol Exp Ther 2000; 294:983-990.
5. Ree P, Burris D, Kaufmann C, Pikoulis M, Austin B et al. Lactate ringer's solution resuscitation causes neutrophil activation after hemorrhagic shock. J Trauma 1998; 44:313-319.
6. Botha AJ, Moore FA, Moore EE, Sauaia A, Banerjee A et al. Early neutrophil sequestration after injury: a pathologic mechanism for multiple organ failure. J Trauma 1995; 39:411-417.
7. Meng ZH, Dyer K, Billiar TR, and Tweardy DJ. Essential role for IL-6 in postresuscitation inflammation in hemorrhagic shock. Am J Physiol Cell Physiol 2001; 280:C343-C351.

Case Report

Kurume Medical Journal, 54, 85-88, 2007

Perioperative Management of Severe Interstitial Pneumonia for Rectal Surgery: A Case Report

KANEATSU HONMA, YASUHISA TANGO*, KENICHI HONMA*
AND HIROHARU ISOMOTO*

Divisions of Operative management and Surgery, Koga Hospital 21,*
Kurume 839-0801, Japan

Received 27 August 2007, accepted 27 November 2007

Summary: This report describes a case of rectal cancer with severe interstitial pneumonia (IP) and chronic pneumothorax. Acute exacerbation of IP is a serious postoperative complication and the consequences are extremely poor. To provide less invasive surgery and to prevent acute exacerbation of the IP, the patient received chemo-radiotherapy for controlling locally advanced tumor following low anterior resection under combined spinal-epidural anesthesia. Adequate epidural analgesia during the postoperative period had been shown and the epidural catheter was removed on the 3rd postoperative day. The patient showed symptoms of intrapelvic abscess due to the anastomotic leakage at 10th postoperative day. In order to avoid complications due to spinal and epidural anesthesia (epidural abscess, meningitis), and to prevent acute exacerbation of the IP, general anesthesia was employed with minimal fraction of inspired oxygen (FIO_2) to perform the colostomy for the anastomotic leakage. The patient recovered without any postoperative respiratory complications. We herein report the successful perioperative management of a rectal cancer patient with severe IP and chronic pneumothorax, with special attention paid to the respiratory functions.

Key words interstitial pneumonia, rectal cancer, operative management

INTRODUCTION

Interstitial pneumonia (IP) is associated with an increased risk of postoperative acute exacerbation [1]. An acute exacerbation of IP is a serious postoperative complication and the consequences are extremely poor. Therefore, a surgeon must do everything possible to prevent an acute exacerbation of IP [2]. We herein report the successful perioperative management of a rectal cancer patient with severe IP and chronic pneumothorax, while paying special attention to the respiratory functions, to less invasive surgery and anesthetic management.

CASE REPORT

A 68-year-old man who was out patient for his IP with chronic pneumothorax was referred to the division of surgery due to rectal cancer. The patient had presented with dyspnea, exhibiting Hugh-Jones grade 4. Fine crackles were audible. The results of pulmonary function testing indicated a pattern of restrictive defects, including a vital capacity (VC) of 1.44 L (44% of predicted VC) and a forced expiratory volume at 1 s (FEV1.0) of 1.42 L (98.6% of forced VC). Arterial blood gas (ABG) analysis data showed a partial pressure of oxygen (PaO_2) of 141.9 torr (99.5% arterial oxygen saturation (SaO_2)), a partial pressure of carbon dioxide ($PaCO_2$) of 42.6 torr, and pH of 7.452 with 1 L

Reprint requests to: K. Honma, Koga Hospital 21, 3-3-8 Miyanojin, Kurume 839-0801, Japan. Tel: 0942-38-3333 Fax: 0942-38-2946 E-mail: khonma@tc5.so-net.ne.jp

Abbreviations: ABG, arterial blood gas; CT, computed tomography; FEV, forced expiratory volume; FIO_2, fraction of inspired oxygen; IP, interstitial pneumonia; $PaCO_2$, partial pressure of carbon dioxide; PaO_2, partial pressure of oxygen; SaO_2, arterial oxygen saturation; SpO_2, pulse oxygen saturation; VC, vital capacity.

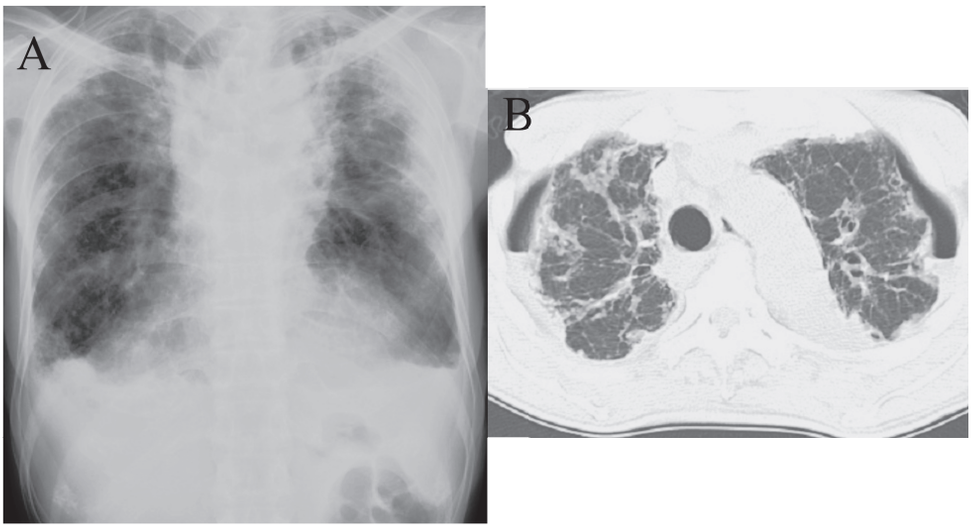

Fig. 1. (A) A chest radiograph on admission showed a diffuse reticular shadow and pleural thickening in both lungs without typical honeycombing. (B) A chest CT (computed tomography) image showed interstitial pneumonia with a reticular shadow without typical honeycombing, thus indicating a fibronodular change and bilateral pneumothorax.

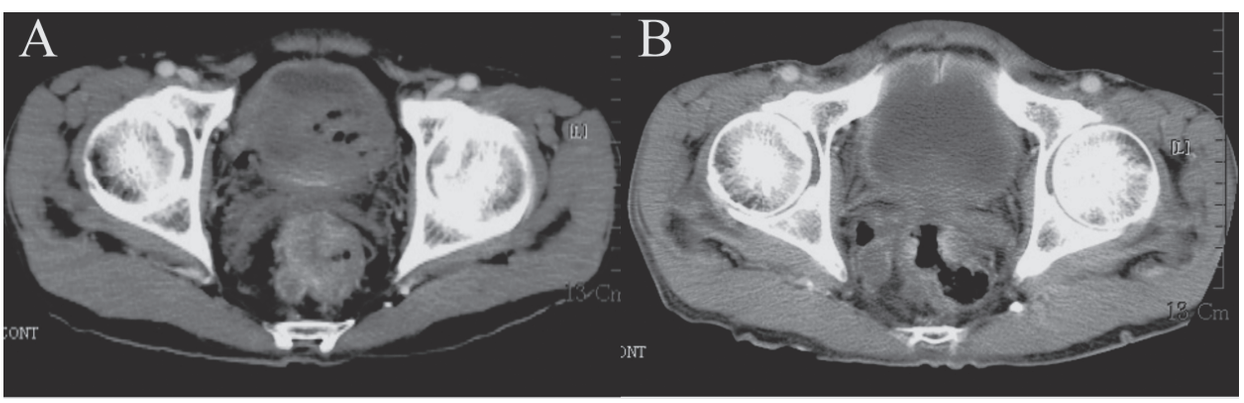

Fig. 2. (A) An abdominal CT showed the wall thickness and the stenosis of the rectum, and the swelling of the pararectal lymph node. (B) The tumor and lymph node were observed to have decreased in size.

of nasal flow of oxygen in the supine position. The serum lactate dehydrogenase level was normal. The major causal factors of secondary IP include such factors, as the occupational history, the residential history, the drug history and the collagen disease were evaluated. The patient was diagnosed to have stable idiopathic IP based on clinical findings, chest X-ray films and chest computed tomography (CT) by chest physicians (Fig. 1). A total of 41.8 Gy radiation therapy for controlling locally advanced tumors was conducted for 4 weeks in the combination with 750 mg of Tegaful suppository for 2 weeks, reduction of the tumor size (partial response) was found (T3, N0, M0: stageⅡ) (Fig. 2), and a low anterior resection was employed under combined spinal-epidural anesthesia in spontaneous respiration in the lithotomic position. An epidural catheter was placed at T10-T11 space. A test dose of 4 ml of 1% lidocaine hydrochloride was given to rule out subarachnoid or intravascular placement of the catheter, and then, spinal anesthesia was initiated by injecting 2.8 ml of 0.5% isobaric lidocaine hydrochloride and 1 ml of fentanyl citrate via a 25 gauge spinal needle into the L3-L4 interspace. Epidural analgesia was continuously injected by 2 ml of 1% lidocaine hydrochloride. Intraoperative sedation was provided with titrated doses (10 ml) of propofol; a total of 550 ml of propofol was given. The surgery lasted 4 hrs. The postoperative epidural analgesia was very satisfactory for managing the pain. ABG analysis on 30% fraction of inspired oxygen (FIO_2) showed 100%

of pulse oxygen saturation (SpO_2) and almost the same PaO_2 as that of preoperative data (PH 7.348, $PaCO_2$ 56.3 torr, PaO_2 147.0 torr intraoperatively). Postoperative ABG analysis was followings, PH 7.412, $PaCO_2$ 48.7 torr, PaO_2 104.5 torr and SpO_2 99% on 1 L of mask flow of oxygen in the supine position. The postoperative respiratory functions were uneventful. About the 10th postoperative day, the patient showed symptoms of intrapelvic abscess due to the anastomotic leakage. In order to avoid complications due to spinal or epidural anesthesia and to prevent acute exacerbation, general anesthesia was employed with minimal FIO_2 (30% of FIO_2 and 1.7% of sevoflurane with intra venous administration of fentanyl citrate, tidal volume 350 L, respiration rate 6-8/min) for the colostomy. The surgery lasted 100 min. ABG data are followings respectively, PH 7.347, $PaCO_2$ 52.7 torr, PaO_2 177.6 torr (intraoperatively), PH 7.438, $PaCO_2$ 43.4 torr, PaO_2 84.9 torr (postoperatively). The perioperative pulmonary functions were normal and no problems were observed.

DISCUSSION

IP is associated with an increased risk of postoperative acute exacerbation [1]. Acute exacerbation of IP is a serious postoperative complication and the consequences are extremely poor. Therefore, a surgeon must aim to prevent an acute exacerbation of IP [2]. In addition, the possibility of pneumothorax due to a rupture of the bullae was an important anesthetic consideration in this patient [3,4]. Even though a lung biopsy or bronchoscopy has been recommended to diagnose IP, the high risk of mortality resulting from an acute exacerbation of IP could not be ignored [5,6]. In this case, we did not perform both a lung biopsy and bronchoscopy. To provide less invasive surgery, the patient received radiotherapy for controlling the locally advanced tumors followed by a low anterior resection under combined spinal-epidural anesthesia in spontaneous respiration. A continuous epidural infusion of fentanyl citrate in 1% lidocaine hydrochloride was used to relieve postoperative pain following the first operation and the postoperative pulmonary functions were uneventful. In order to avoid complications such as epidural abscess, meningitis, and to prevent acute exacerbation and rupture of bulla, general anesthesia was employed with minimal FIO_2 (0.3-0.4) at the 2nd operation because the patient's condition was thought to be bacteremia. The SpO_2 was 100% after intubation. Ventilation consisted of a tidal volume of 350 ml, and a respiratory rate of 6 to 8 breaths/min. The perioperative respiratory functions were uneventful without any pulmonary complications. In this case, there was concern about anastomotic leakage because of the poor condition of the patient, the influence of radiotherapy, and the low colorectal anastomosis, which would require a temporary colostomy to reduce postoperative complications [7].

Seven of 47 lung cancer patients showed an acute exacerbation of IP within 30 days after undergoing video-assisted less invasive thoracic surgery [8]. There was no correlation between the surgical invasiveness and the postoperative complications of the IP [9-11]. However, clinical deterioration in IP is expected and the 5 year survival ranges from 30 to 50%. In addition, few studies have identified the features of IP that are associated with an increased risk of disease progression and death [12,13]. It is possible that one of these factors would restrict major surgery.

Since the high concentration of oxygen is suggested to be one of the causes of the postoperative exacerbation of IP, when a patient received an operation under general anesthesia, minimal FIO_2 must be used with the general anesthesia [9-11,14]. However, the correlation between the high concentration of oxygen and acute exacerbation is controversial and inadequately defined [8,10]. Clark and Lanbertsten [15] reviewed the toxic effects of oxygen upon the lung and the mechanisms of pulmonary oxygen toxicity. These results suggested that intraoperative oxygen concentration should be reduced as much as possible [9,10,14,16].

It was difficult to predict the development acute exacerbation of IP [11,14], further studies to investigate the correlation between acute exacerbation and intraoperative FIO_2 in cooperation with an anesthesiologist are needed. For the perioperative administration to prevent an acute exacerbation, methylprednisolone and bronchodilators may be useful [17]. In addition, the presence of inflammation might contribute to acute lung tissue damage and exacerbation. We should avoid surgery in patients demonstrating the presence of inflammation or an active phase of IP. In conclusion, this report documents the successful perioperative management of IP with chronic pneumothorax during rectal surgery. For major surgery for a patient with severe IP, the selection of appropriate therapy under the evaluation of activity of IP, the careful observation of respiratory state after surgery and the cooperation between surgeons and anesthesiologists in order to perform less invasive surgery and prevent postoperative acute exacerbation is thus considered to be important.

REFERENCES

1. Kumar P, Goldstraw P, Yamada K, Nicholson AG, Walls AU et al. Pulmonary fibrosis and lung cancer: risk and benefit analyses of pulmonary resection. J Thorac Cardiovasc Surg 2003; 125:1321-1327.
2. American Thoracic Society and European Respiratory Society. Idiopathic pulmonary fibrosis: diagnosis and treatment. International consensus statement. Am J Respir Crit Care Med 2000; 161:646-664.
3. Picado C, Gomez de Almedia R, Xaubet A, Montserrat J, Letang E et al. Spontaneous pneumothorax in cryptogenic fibrosing alveolitis. Respiration 1985; 48:77-80.
4. Trikha A, Sadhasivam S, Saxena A, and Aora MK. Thoracic epidural anesthesia for modified radical mastectomy in a patient with cryptogenic fibrosing alveolitis: A case report. J Clin Anesth 1999; 12:75-79.
5. Amemiya T, Nishi K, Mizuguchi M, Ohka T, Kurumaya H et al. A case of acute type idiopathic interstitial pneumonia associated with acute exacerbation induced by bronchoalveolar lavage. JJSB 1995; 17:80-86.
6. Enomoto T, Kawamoto M, Kunugi S, Hiramatsu K, Sakakibara K et al. Clinichopathological analysis of patients with idiopathic pulmonary fibrosis which became acutely exacerbated after video-assisted thoracoscopic surgical lung biopsy. JJRS 2002; 40:806-811.
7. McNamara DA, and Parc R. Methods and results of sphincter-preserving surgery for rectal cancer. Cancer Control 2003; 3:212-218.
8. Koizumi K, Hirata T, Hirai K, Mikami I, Okada D et al. Surgical treatment of lung cancer combined with interstitial pneumonia: The effect of surgical approach on postoperative acute exacerbation. Ann Thorac Surg 2004; 6:340-346.
9. Tanimura S, Tomoyasu H, Banba J, Masaki M, Nakada K et al. A clinical analysis of surgical cases of lung cancer complicated with idiopathic pneumonia. Nitikyo (Jpn J Chest Dis) 1992; 3:208-213. (in Japanes)
10. Tsuchida M, Yamato Y, Souma T, Yoshiya K, Aoki T et al. Perioperative management of patients with lung cancer associated with interstitial pneumonia. Haigan (JJLC) 1999; 7:995-1000. (in Japanese)
11. Okada D, Koizuni K, Kawamoto M, Henmi S, Hirai K et al. Clinicopathologic considerations of postoperative acute exacerbation in patients with idiopathic interstitial pneumonia combined with lung cancer: Haigan (JJLC) 2002; 6:567-572. (in Japanese)
12. Bjoraker JA, Ryu JH, Edwin MK, Myers JL, Tazelaar HD et al. Prognostic significance of histopathologic subsets in idiopathic pulmonary fibrosis. Am J Respir Crit Care Med 1998; 157:199-203.
13. Schwartz DA, Van Fossen DS, Davis CS, Helmers RA, Dayton CS et al. Determinants of progression in idiopathic pulmonary fibrosis. Am J Respir Crit Care Med 1994; 149:444-449.
14. Goldiner PL, and Schweizer O. The hazards of anesthesia and surgery in bleomycin-treated patients. Seminars in Oncology 1979; 1:121-124.
15. Clark JM, and Lambersten CJ. Pulmonary oxygen toxicity: a review. Pharmacol Rev 1971; 23:37-133.
16. Edmark L, Aherdan KK, Enlund M, and Hedenstierna G. Optimal oxygen concentration during induction of general anesthesia. Anesthesiology 2003; 98:28-33.
17. Kondo A. Drug treatment for interstitial pneumonia. ICU&CCU 1994; 18:875-885.

Case Report

Kurume Medical Journal, 54, 89-93, 2007

A Case of Horseshoe Kidney with Surplus Renal Arteries

AKIRA YAKEISHI*,**, TSUYOSHI SAGA*, HIROKO SO*, MAKOTO TETSUKA*, YOSHIO ARAKI*, SEIJI KOBAYASHI* AND KOH-ICHI YAMAKI*

Department of Anatomy and Dental and Oral Medical Center**, Kurume University School of Medicine, Kurume 830-0011, Japan*

Received 4 October 2007, accepted 17 December 2007

Edited by SEIYA OKUDA

Summary: During a gross anatomy course at Kurume University School of Medicine in 2001, an anomaly of the kidneys was found. The lower ends of the kidneys were fused by a renal substance and formed a horseshoe kidney located ventral to the abdominal aorta and inferior vena cava. Both renal hila opened very widely in the ventral direction, with the left hilum being larger than the right. This horseshoe kidney had original left and right renal arteries that branched from the abdominal aorta. As well, there were four surplus renal arteries. The first surplus artery branched from the right renal artery and was distributed to the upper pole of the right kidney. The second arose from the abdominal aorta and was distributed to the inferior pole of the right kidney. The third arose from the abdominal aorta and was distributed to the inferior pole of the left kidney and part of the isthmus. The fourth branched from the abdominal aorta and was distributed to the upper pole of the left kidney. The incidence of horseshoe kidneys in Japanese anatomical dissections has been reported as 0.15-0.48%. This was the sixth such case for our laboratory, representing a frequency of 0.1% (6 of 1902 dissections) from 1952 to 2001.

Key words human anatomy, anomaly, horseshoe kidney

INTRODUCTION

The horseshoe kidney is a well known congenital fusion anomaly of the kidneys. The frequency of horseshoe kidney incidence ranges from 1/400 to 1/1800 [1]. During the gross anatomy course at Kurume University School of Medicine in 2001, the sixth case of horseshoe kidney was found in our laboratory. This horseshoe kidney had a tumor mass on the left upper side of the isthmus and a rare arterial anomaly of the celiac trunk.

CASE REPORT

This report describes an kidney anomaly found in an 81-year-old Japanese male cadaver who had died of bladder cancer. The lower ends of the kidneys were fused and thus formed a horseshoe kidney. The horseshoe kidney was located ventral to the abdominal aorta and inferior vena cava. A huge tumor mass was present on the left side of the isthmus to the upper pole of the left kidney with accretion. After removal of the tumor mass, the boundaries between the isthmus and the kidneys were indistinct. The long axes of both kidneys ran from the outer upper side to the inner lower side. The surfaces of the kidneys were smooth (Fig. 1 A and B).

Size and position of the horseshoe kidney

The upper poles of the left and right kidneys were positioned at the level between the first and second lumbar vertebrae. The upper edge of the isthmus was at the level of the third lumbar vertebra. The lower edge of the isthmus was at the level between the fourth

Corresponding Author: Akira Yakeishi, Department of Anatomy, Kurume University School of Medicine, 67 Asahi-machi, Kurume 830-0011, Japan. Tel: +81-942-31-7540 Fax: +81-942-33-3233 E-mail: yakeishi@med.kurume-u.ac.jp

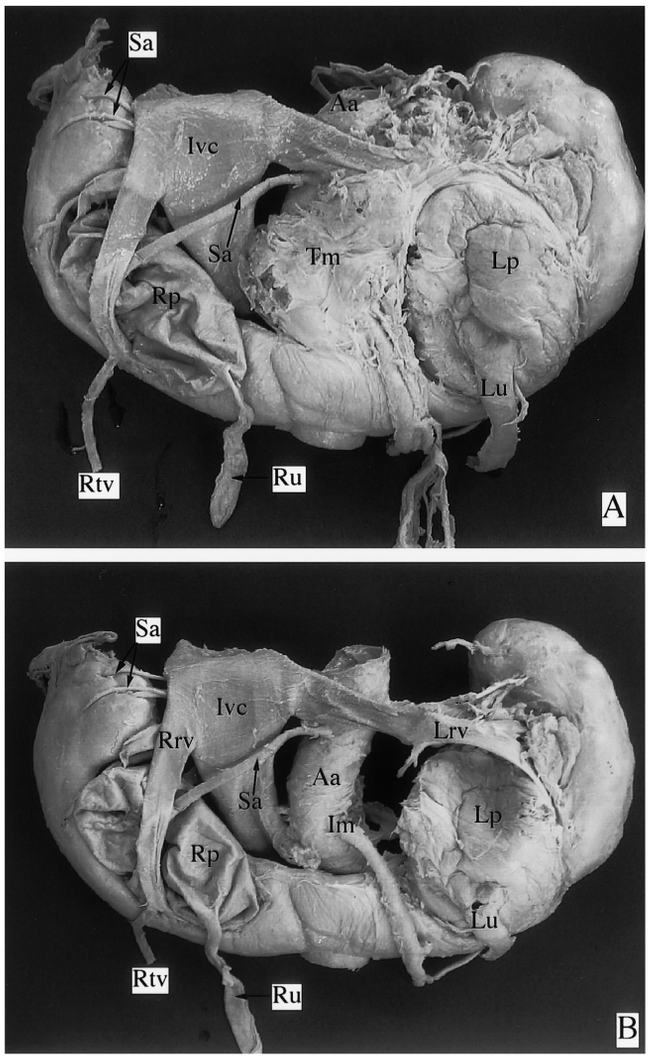

Fig. 1. A. Photograph showing the horseshoe kidney and its arterial system and venous system including a tumor, as viewed from the ventral side. B. Photograph showing the horseshoe kidney and its arterial system and venous system after the tumor removal, as viewed from the ventral side. Aa, abdominal aorta; Im, inferior mesenteric artery; Ivc, inferior vena cave; Lp, left pelvis; Lrv, left renal vein; Lu, left ureter; Rp, right pelvis; Ru, rightureter; Rrv, right renal vein; Rtv, right testicular vein; Sa, surplus Artery; Tm, tumor.

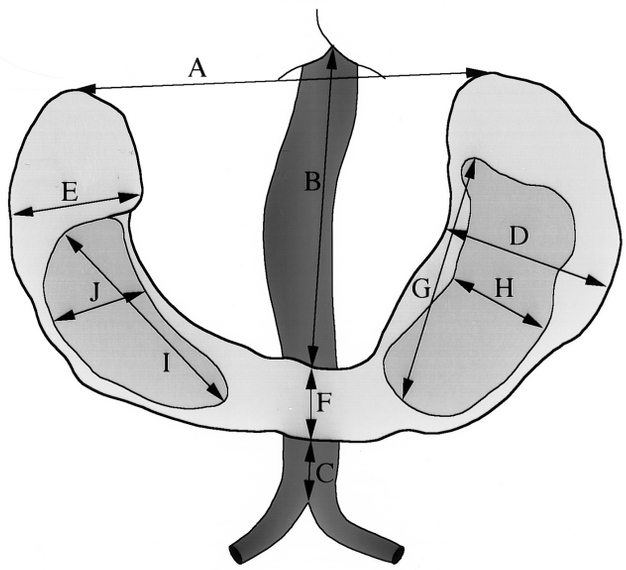

Fig. 2. Various measurements of the horseshoe kidney. The result of the measurements are shown in Table 1. A. Distance between the tops of the left and right kidneys. B. Distance between the aortic hiatus and the top edge of the isthmus. C. Distance between the lower edge of the isthmus and the divergent Points of the common iliac arteries. D. Width of the left kidney. E. Width of the right kidney. F. Width of the isthmus. G. Major axis of the hilum of the left kidney. H. Minor axis of the hilum of the left kidney. I. Major axis of the hilum of the right kidney. J. Minor axis of the hilum of the right kidney.

TABLE 1.
Results of the measurements of each region shown in Fig. 2

Regions	(cm)	Regions	(cm)
A	13.1	F	3.1
B	6.3	G	6.9
C	2.5	H	3.9
D	6.0	I	7.3
E	4.3	J	2.8

and fifth lumber vertebrae. The sizes of the kidneys and the lengths of each section were measured (Fig. 2 and Table. 1).

Renal hilum, pelvis and ureter

Both renal hila opened very widely in the ventral direction, and the left hilum was larger than the right hilum. The right pelvis consisted of six major calyces, while the left pelvis was enlarged because of the tumor. The left calyces could not be observed clearly due to the tumor. Both ureters descended from the ventral side of each kidney and penetrated normally into the bladder.

Arterial system

After passing through the aortic hiatus of the diaphragm, the aorta descended, turned slightly to the right and passed through the dorsal side of the isthmus of the horseshoe kidney. Subsequently, it diverged into the left and right common iliac arteries. The arterial system of this horseshoe kidney is shown in Fig. 3 A

and B. The left and right renal arteries branched from the abdominal aorta. Moreover, a surplus arteries from the renal arteries and three surplus arteries from the abdominal aorta penetrated into the horseshoe kidney. The first surplus artery branched from the right renal artery and became distributed to the upper pole of the right kidney. The second surplus artery arose from the ventral side of the aorta below the origin of the superior mesenteric artery and became distributed to the inferior pole of the right kidney. The third surplus artery arose from the ventral side of the abdominal aorta below the origin of the inferior mesenteric artery and became distributed to the inferior pole of the left kidney and part of the isthmus. The fourth surplus artery branched from the left side of the abdominal aorta superior to the origin of the left renal artery and became distributed to the upper pole of the left kidney (Fig. 3 B).

Moreover, the usual celiac trunk was not identified in the present case. The splenic artery arose from the superior mesenteric artery, forming a lienomesenteric trunk, and the left gastric and common hepatic arteries, forming a gastrohepatic trunk.

Venous system

The inferior vena cava formed from the junction of the right and left common iliac veins. It ascended to the right side of the abdominal aorta behind the isthmus. In the left kidney, two veins arose from the left hilum and joined into one vein that opened into the inferior vena cava. In the right kidney, two veins arose from the right hilum and joined into one vein that opened into the inferior vena cava. Other surplus veins arose the right hilum and directly opened into inferior vena cava.

Histological observation of isthmus

In order to observe the tissue of the isthmus, some paraffin-embedded preparations of part of the isthmus were stained with H&E. Many renal corpuscles and renal tubules were observed in this area (Fig. 4). The isthmus consisted of kidney substance in the present case.

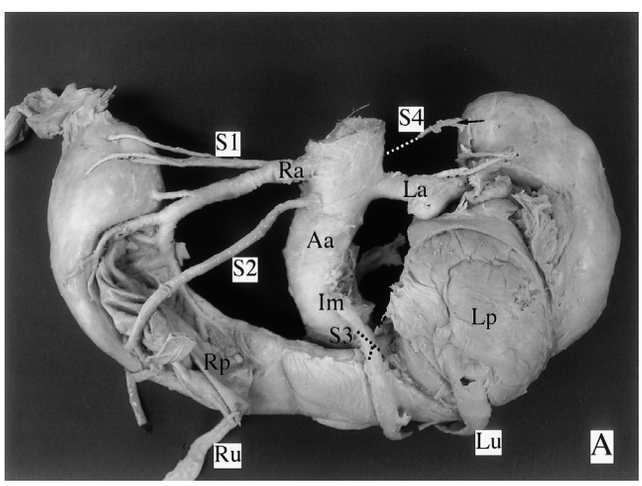

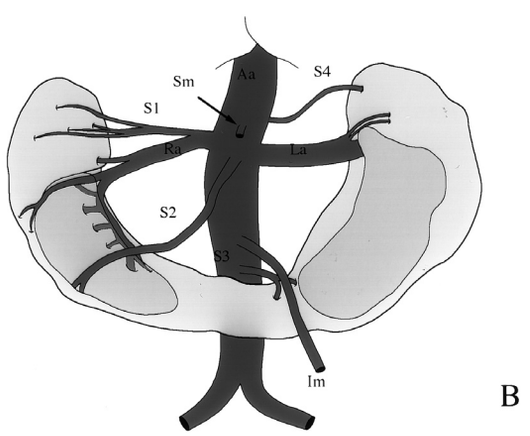

Fig. 3. A. Photograph showing the horseshoe kidney and its arterial system, as viewed from the ventral side. One surplus artery (S3) arises from the abdominal aorta behind the inferior mesenteric artery. B. Schematic diagram of the distribution of the arteries to the kidney. Aa, abdominal aorta; Sm, superior mesenteric artery; Im, inferior mesenteric artery; La, left renal artery; Lp, left pelvis; Lu, left ureter; Ra, right renal artery; Rp, right pelvis; Ru, right ureter; S1-S4, surplus arteries.

DISCUSSION

A horseshoe kidney is the most frequent disease among dysraphia of kidney. The incidence of horse-

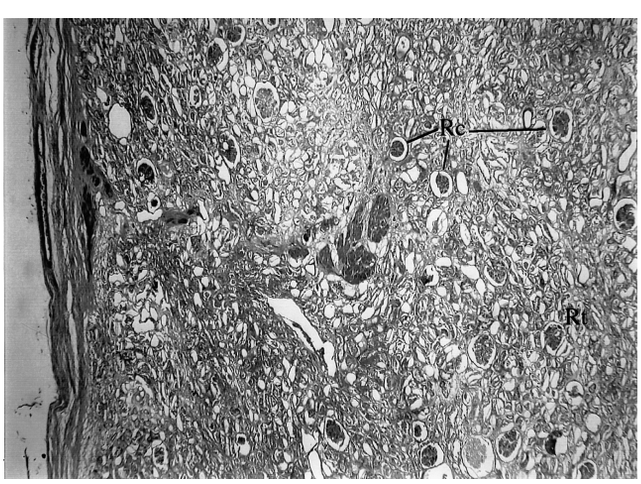

Fig. 4. Light microscopic photograph of the isthmus of this horseshoe kidney. Many renal corpuscles (Rc) and renal tubules (Rt) are existed. (HE ×30)

shoe kidneys in Japanese is 0.15-0.48% [1-3]. Sex differences are seen, similar to other types of dysraphia, and men are twice as likely to have a horseshoe kidney than women [1,4,5]. This is the sixth case in our laboratory, representing a frequency of 0.1% (6 of 1902 bodies) from 1952 to 2001 [6].

Matsumoto et al. [2] classified horseshoe kidneys into the following five types: type A(a), fused at the superior poles; type A(b), fused at the inferior poles; type B(a), fused by fibrous tissue; type B(b), fused directly; and type B(c), fused by mediators. In the present case, the isthmus consisted of kidney substance and the extremitas inferior of both kidneys carried out the coalescence. Therefore, this case of horseshoe kidney belongs to types A(b) and B(b). Although the coalescence part is the inferior poles of the kidneys in 95% of cases, a case in which the upper poles carried out the coalescence has also been reported [7]. Similar to many old reports, in this example, the hilum opened ahead greatly [8-15].

Embryologically, the generation of a normal kidney begins in the 4-week-old embryo when the tail side of the primordial kidney upheaval carries out a coalescence to a metanephric bud, and a metanephric tissue is formed. The metanephric tissue progressively moves to the head side as the fetus grows and the pelvic organs progress. The kidneys ascended over the iliac crest in the 7-week-old embryo, and almost reach their final positions in the 9-week-old embryo. When moving in the upward direction, the kidney rotates so that the ventral aspect may be suitable inside. It is supposed that abnormalities in the coalescence of a kidney are produced when the early fetal renal capsule is still premature and the kidney is moving in the pelvis. The time when the two kidneys approach each other most closely is when they pass through the umbilical artery and get over the common iliac artery in the 4-6-week-old embryo. Therefore, when the position of these blood vessels is slightly unusual or the sacrum and coccyx are crooked on the right or left, coalescence of a kidney arises [16]. It is most likely that the inferior poles of both kidneys carry out a coalescence and form a horseshoe kidney at this time. Since such a fusion is previously produced as a kidney rotates around the long axis as the center, the renal pelvis has turned toward the ventral aspect. However, according to a recent report on 6-7-week-old embryos, the coalescence produced when the left and right kidneys merely approach each other is only applicable to some horseshoe kidneys, in which a bridge part arises from a fibroid organization, and the view that both kidneys carry out the coalescence, since the dorsal metanephric tissue showed excrescence in most cases, which have a bridge part of substance nature, is also presented [10,17].

There are many opinions that the surplus arteries observed as features of horseshoe kidneys are vestigial remnants of an embryo term [9,12,18,19]. There are many views about the cause, in which a kidney is fixed too low because the rise of the kidney is barred by the surplus arteries [13,15] and also barred by the origin of the inferior mesenteric artery or abnormal growth of the early developmental renal tissue [14,15,20].

Moreover, horseshoe kidneys show great individual arterial variations, and this is supposed to be accompanied by variation in the branches of the abdominal aorta in many cases [5]. In the present case, a rare arterial anomaly was observed in the celiac mesenteric region. The usual celiac trunk was not identified, and the gastrohepatic trunk and splenomesenteric trunk independently arose from the abdominal aorta. The classification for this type of arterial anomaly is type V''' in Morita's classification, but does not belong to Adachi's classification [21,22].

REFERENCES

1. Bauer SB, Perlmutter AD, and Retik AB. Anomales of the upper urinary tract, horseshoe kidney. In: Campbell's Urology, 6th edn. eds. Walsh PC, Retik AB, Stamey TA, Vaughan ED. WB Saunders, Philadelphia, pp 1376-1381, 1992.
2. Matsumoto T, Arihara K, Oda K, and Inoue K. Case of malformation and variation observed at the dissection practice. (VI) A case of the horseshoe kidney. J Kansai Med Coll 1963; 15:182-188. (in Japanese)
3. Sone T, and Tamura K. A case of the horseshoe kidney. Iwate Ika Daigak Kaibougaku Kyoshitsu Gyosekisyu 1962; 10:85-88. (in Japanese)
4. Nation EF. Horseshoe kidney. A study of thirty-two autopsy and nine surgical cases. J Urol 1945; 53:726.
5. Campbell MF. Anomalies of the kidney. Urology, eds. Campbell MF, and Harrison JH, WB Saunders, Philadelphia, pp 1447-1452, 1970.
6. Aida K, Saga T, Yamaki K, Doi Y, Yoshizuka M et al. A Case of Horseshoe Kidney. Kurume Med J 1997; 44:153-156.
7. Love L, and Wasserman D. Massive unilateral nonfunctioning hydronephrosis in horseshoe kidney. Clin Radiol 1975; 26:409.
8. Yoshinaga K, Kodama K, Tanii I, and Toshimori K. Morphological study of a horseshoe kidney with special reference to the vascular system. Anatomical Science Internationl 2002; 77:134-139.
9. Boyden EA. Description of a horseshoe kidney associated with left inferior vena cava and disc-shaped suprarenal glands, together with a note on the occurrence of horseshoe kidneys in human embryos. Anat Rec 1931; 51:187-211.

10. Domenech-Mateu JM, and Gonzalez-Compta X. Horseshoe kidney: a new theory on its embryogenesis based on the study of a 16-mm human embryo. Anat Rec 1988; 222:408-417.
11. Fuyuta M, Ukeshima A, and Miyayama Y. An autopsy case of horseshoe kidney. Okajimas Fol Anat Jpn 1977; 53:323-336.
12. Graves FT. The arterial anatomy of the kidney. John Wright & Sons, Bristol, England 1971.
13. Honjin R, and Osugi H. A case of the horseshoe kidney. Juzenkai Z 1955; 57:2160-2164. (in Japanese)
14. Isomura G, Kubo K, and Uematsu H. Ramified pelves and their blood supply of the horseshoe kidney in 2 Japanese. Anat Anz 1988; 167:393-402.
15. Takeshige Y, Takaoka T, Yasunari T, and Abiru M. A case of Horseshoe Kidney. Kurumeigakukai Z 1966; 29:540-549. (in Japanese)
16. Shimada K, Hosokawa S, and Tohda A. Horseshoe Kidney. Jpn J Pediatr Surg 1992; 24:1233-1237.
17. Shimada K, Hosokawa S, and Higashida A. Horseshoe Kidney. Shounigeka 1992; 24:11. (in Japanese)
18. Boyden EA. Congenital absence of the kidney. An interpretation based on a 10-mm. Human embryo exhibiting unilateral renal agenesis. Anat Rec 1932; 52:325-339.
19. Bremer JL. The origin of the renal artery in mammals and its anomalies. Am J Anat 1915; 18:179-200.
20. Lewis FT, and Papez JW. Variation in the early development of the kidney in pig embryos with reference to the production of anomalies. Anat Rec 1915; 9:105-106.
21. Morita M. Reports and conception of three anomalous case in the area of the celiac and the superior mesenteric arteries. Igaku Kenkyu 1935; 9:1993-2006. (in Japanese)
22. Adachi B. Das Arteriensystem der Japaner. Die Kaiserlich Japanische Universitat zu Kyoto 1928; Bd:1.